CERN-PH-EP-2011-097
Submitted to Physical Review D

Measurement of the $Z \to \tau\tau$ Cross Section with the ATLAS Detector

The ATLAS Collaboration*
(Dated: October 24, 2011)

The $Z \to \tau\tau$ cross section is measured with the ATLAS experiment at the LHC in four different final states determined by the decay modes of the τ leptons: muon-hadron, electron-hadron, electron-muon, and muon-muon. The analysis is based on a data sample corresponding to an integrated luminosity of 36 pb^{-1}, at a proton-proton center-of-mass energy of $\sqrt{s} = 7$ TeV. Cross sections are measured separately for each final state in fiducial regions of high detector acceptance, as well as in the full phase space, over the mass region $66 - 116$ GeV. The individual cross sections are combined and the product of the total Z production cross section and $Z \to \tau\tau$ branching fraction is measured to be 0.97 ± 0.07 (stat) ± 0.06 (syst) ± 0.03 (lumi) nb, in agreement with NNLO calculations.

PACS numbers: 13.38.Dg, 13.85.Qk

I. INTRODUCTION

Tau leptons play a significant role in the search for new physics phenomena at CERN's Large Hadron Collider (LHC). Hence decays of Standard Model gauge bosons to τ leptons, $W \to \tau\nu$ and $Z \to \tau\tau$, are important background processes in such searches and their production cross sections need to be measured precisely. Studies of $Z \to \tau\tau$ processes at the LHC center-of-mass energies are also interesting in their own right, complementing the measurements of the Z boson through the electron and muon decay modes. Finally, measuring the cross section of a well-known Standard Model process involving τ leptons is highly important for the commissioning and validation of τ identification techniques, which will be crucial for fully exploiting the ATLAS experiment's potential in searches for new physics involving τ leptons.

This paper describes the measurement of the $Z \to \tau\tau$ cross section, using four different final states and an integrated luminosity of 36 pb^{-1}, in pp collisions at a center-of-mass energy of $\sqrt{s} = 7$ TeV recorded with the ATLAS detector [1] at the LHC. Two of the considered final states are the semileptonic modes $Z \to \tau\tau \to \mu + \text{hadrons} + 3\nu$ ($\tau_\mu\tau_h$) and $Z \to \tau\tau \to e + \text{hadrons} + 3\nu$ ($\tau_e\tau_h$) with branching fractions $(22.50 \pm 0.09)\%$ and $(23.13 \pm 0.09)\%$ respectively [2]. The remaining two final states are the leptonic modes $Z \to \tau\tau \to e\mu + 4\nu$ ($\tau_e\tau_\mu$) and $Z \to \tau\tau \to \mu\mu + 4\nu$ ($\tau_\mu\tau_\mu$) with branching fractions $(6.20 \pm 0.02)\%$ and $(3.01 \pm 0.01)\%$, respectively [2]. Due to the large expected multijet background contamination, the $\tau_h\tau_h$ and $\tau_e\tau_e$ final states are not considered in this publication.

The $Z \to \tau\tau$ cross section has been measured previously in $p\bar{p}$ collisions at the Tevatron using the semileptonic τ decay modes [3, 4]. More recently the cross section, using both the semileptonic and leptonic modes, was measured in pp collisions at the LHC by the CMS Collaboration [5].

After a brief description of the ATLAS detector in Section II, the data and Monte Carlo samples are presented in Section III. The object and event selections are detailed in Section IV. The estimation of the backgrounds is described in Section V. The calculation of the cross sections is outlined in Section VI, and a discussion of the systematic uncertainties is given in Section VII. The results, including the combination of the four channels, are presented in Section VIII.

II. THE ATLAS DETECTOR

The ATLAS detector [1] is a multi-purpose apparatus operating at the LHC, designed to study a range of physics processes as wide as possible. ATLAS consists of several layers of subdetectors – from the interaction point outwards, the inner detector tracking system, the electromagnetic and hadronic calorimeters, and the muon system.[1]

The inner detector is immersed in a 2 T magnetic field generated by the central solenoid. It is designed to provide high-precision tracking information for charged particles and consists of three subsystems, the Pixel detector, the Semi-Conductor Tracker (SCT), and the Transition Radiation Tracker (TRT). The first two subsystems cover a region of $|\eta| < 2.5$ in pseudorapidity, while the TRT reaches up to $|\eta| = 2.0$. A track in the barrel region typically produces 11 hits in the Pixel and SCT detectors and 36 hits in the TRT.

* Full author list given at the end of the article.

[1] ATLAS uses a right-handed coordinate system with its origin at the nominal interaction point (IP) in the center of the detector and the z-axis along the beam pipe. The x-axis points from the IP to the center of the LHC ring, and the y axis points upward. Cylindrical coordinates (r, ϕ) are used in the transverse plane, ϕ being the azimuthal angle around the beam pipe. The pseudorapidity is defined in terms of the polar angle θ as $\eta = -\ln\tan(\theta/2)$. The distance ΔR in the $\eta - \phi$ space is defined as $\Delta R = \sqrt{(\Delta\eta)^2 + (\Delta\phi)^2}$.

The electromagnetic (EM) and hadronic calorimeters cover the range $|\eta| < 4.9$, with the η region matched to the inner detector having a finer granularity in the EM section, needed for precision measurements of electrons and photons. The EM calorimeter uses lead as an absorber and liquid argon (LAr) as the active material. The hadronic calorimeter uses steel and scintillating tiles in the barrel region, while the end-caps use LAr as the active material and copper as the absorber. The forward calorimeter also uses LAr as the active medium with copper and tungsten absorbers.

The muon spectrometer relies on the deflection of muons as they pass through the magnetic field of the large superconducting air-core toroid magnets. The precision measurement of muon track coordinates in the bending direction of the magnetic field is provided, over most of the η-range, by Monitored Drift Tubes (MDT). Cathode Strip Chambers (CSC) are used in the innermost plane for $2.0 < |\eta| < 2.7$ due to the high particle rate in that region. The muon trigger, as well as the coordinate in the direction orthogonal to the bending plane, are provided by Resistive Plate Chambers (RPC) in the barrel and Thin Gap Chambers (TGC) in the end-caps.

The ATLAS detector has a three-level trigger system consisting of Level-1 (L1), Level-2 (L2), and the Event Filter (EF).

At design luminosity the L1 trigger rate is approximately 75 kHz. The L2 and EF triggers reduce the event rate to approximately 200 Hz before data transfer to mass storage.

III. DATA AND MONTE CARLO SAMPLES

The data sample used in this analysis corresponds to a total integrated luminosity of about 36 pb^{-1}, recorded with stable beam conditions and a fully operational detector in 2010.

Events are selected using either single-muon or single-electron triggers with thresholds based on the transverse momentum (p_{T}) or transverse energy (E_{T}) of the muon or electron candidate, respectively. For the $\tau_\mu\tau_h$ and $\tau_\mu\tau_\mu$ final states, single-muon triggers requiring $p_{\mathrm{T}} > 10-13$ GeV, depending on the run period, are used. For the $\tau_e\tau_h$ and $\tau_e\tau_\mu$ final states, a single-electron trigger requiring $E_{\mathrm{T}} > 15$ GeV is used. In the $\tau_e\tau_\mu$ final state the choice was made to use a single-electron trigger rather than a single-muon trigger because it is more efficient, as well as allowing a low offline p_{T} cut on the muon.

The efficiency for the muon trigger is determined from data using the so-called "tag-and-probe method", applied to $Z \to \mu\mu$ events. It is found to be close to 95% in the end-cap region, and around 80% in the barrel region (as expected from the geometrical coverage of the RPC).

Similarly, the electron trigger efficiency is measured in data, using $W \to e\nu$ and $Z \to ee$ events. It is measured to be $\sim 99\%$ for offline electron candidates with $E_{\mathrm{T}} > 20$ GeV and $\sim 96\%$ for electron candidates with E_{T} between 16 and 20 GeV [6].

The signal and background Monte Carlo (MC) samples used for this study are generated at $\sqrt{s} = 7$ TeV with the default ATLAS MC10 tune [7] and passed through a full detector simulation based on the GEANT4 program [8]. The inclusive W and γ^*/Z signal and background samples are generated with PYTHIA 6.421 [9] and are normalized to NNLO cross sections [10].

For the $t\bar{t}$ background the MC@NLO generator is used [11], while the diboson samples are generated with HERWIG [12].

In all samples the τ decays are modeled with TAUOLA [13]. All generators are interfaced to PHOTOS [14] to simulate the effect of final state QED radiation.

IV. SELECTION OF $Z \to \tau\tau$ CANDIDATES

The event preselection selects events containing at least one primary vertex with three or more associated tracks, as well as aiming to reject events with jets or τ candidates caused by out-of-time cosmic-rays events or known noise effects in the calorimeters.

In the case of the two semileptonic decay modes, events are characterized by the presence of an isolated lepton[2] and a hadronic τ decay[3]. The latter produces a highly collimated jet in the detector consisting of an odd number of charged hadrons and additional calorimetric energy deposits from possible π^0 decay products. The two leptonic decay modes are characterized by two isolated leptons of typically lower transverse momentum than those in $Z \to ee/\mu\mu$ events. Finally, in all four channels missing energy is expected from the neutrinos produced in the τ decays. This analysis depends therefore on many reconstructed objects: electrons, muons, τ candidates, jets and missing transverse momentum, $E_{\mathrm{T}}^{\mathrm{miss}}$.

A. Reconstructed Physics Objects

1. Muons

Muon candidates are formed by associating muon spectrometer tracks with inner detector tracks after accounting for energy loss in the calorimeter [15]. A combined transverse momentum is determined using a statistical combination of the two tracks and is required to be greater than 15 GeV for the $\tau_\mu\tau_h$ final states and 10 GeV for the $\tau_e\tau_\mu$ and $\tau_\mu\tau_\mu$ final states. Muon candidates are also required to have $|\eta| < 2.4$ and a longitudinal impact

[2] In the following, the term "lepton", ℓ, refers to electrons and muons only.

[3] In the following, reconstructed jets identified as hadronic τ decays are referred to as "τ candidates" or τ_h.

parameter of less than 10 mm with respect to the primary vertex. In the final muon selection, the combined muon tracks are also required to pass several inner detector track quality criteria [16], resulting in an efficiency of $\sim 92\%$, as measured in data using $Z \to \mu\mu$ events.

2. Electrons

Electron candidates are reconstructed from clusters in the EM calorimeter matched to tracks in the inner detector. Candidate electrons are selected if they have a transverse energy $E_{\mathrm{T}} > 16$ GeV and are within the rapidity range $|\eta| < 2.47$, excluding the transition region, $1.37 < |\eta| < 1.52$, between the barrel and endcap calorimeters. For the $\tau_e\tau_\mu$ final state, the candidates are required to pass the "medium" identification requirements based on the calorimeter shower shape, track quality, and track matching with the calorimeter cluster as described in [15]. The resulting efficiency is $\sim 89\%$. For the $\tau_e\tau_h$ final state, the electron candidate is instead required to pass the "tight" identification criteria, with an efficiency of $\sim 73\%$. In addition to the "medium" criteria, the "tight" selection places more stringent requirements on the track quality, the matching of the track to the calorimeter cluster, the ratio between the calorimeter energy and the track momentum, and the transition radiation in the TRT [15]. The electron reconstruction and identification efficiencies are measured in data using $W \to e\nu$ and $Z \to ee$ events.

3. Jets

The jets used in this analysis are reconstructed using the anti-k_{T} algorithm [17], with a distance parameter $R = 0.4$, using three-dimensional topological calorimeter energy clusters as inputs. The energy of the jets is calibrated using p_{T} and η-dependent correction factors [18] based on simulation and validated by test beam and collision data. Jet candidates are required to have a transverse momentum $p_{\mathrm{T}} > 20$ GeV and a rapidity within $|\eta| < 4.5$.

4. Hadronic τ candidates

The reconstruction of hadronic τ decays is seeded by calorimeter jets. Their energy is determined by applying a MC-based correction to the reconstructed energy in the calorimeters. Tracks with $p_{\mathrm{T}} > 1$ GeV passing minimum quality criteria are associated to calorimeter jets to form τ candidates. Reconstructed τ candidates are selected if they have a transverse momentum $p_{\mathrm{T}} > 20$ GeV and lie within the pseudorapidity range $|\eta| < 2.47$, excluding the calorimeter transition region, $1.37 < |\eta| < 1.52$. Further, a τ candidate is required to pass identification selection criteria, based on three variables describing its energy-weighted transverse width in the electromagnetic calorimeter (R_{EM}), its p_T-weighted track width (R_{track}), and the fraction of the candidate's transverse momentum carried by the leading track. In order to account for the increasing collimation of the τ candidates with increasing p_{T}, the selection criteria on the quantities R_{EM} and R_{track} are parametrized as a function of the p_{T} of the τ candidate. The identification is optimized separately for candidates with one or multiple tracks. Additionally, a dedicated selection to reject fake τ candidates from electrons is applied. This leads to an efficiency of $\sim 40\%$ ($\sim 30\%$) for real 1 prong (3 prong) τ candidates as determined from signal Monte Carlo [19]. For fakes from multijet final states the efficiency is $\sim 6\%$ ($\sim 2\%$) for 1 prong (3 prong) candidates, as measured in data using a dijet selection [20].

5. Missing transverse momentum

The missing transverse momentum ($E_{\mathrm{T}}^{\mathrm{miss}}$) reconstruction used in all final states relies on energy deposits in the calorimeter and on reconstructed muon tracks. It is defined as the vectorial sum $E_{\mathrm{T}}^{\mathrm{miss}} = E_{\mathrm{T}}^{\mathrm{miss}}(\mathrm{calo}) + E_{\mathrm{T}}^{\mathrm{miss}}(\mathrm{muon}) - E_{\mathrm{T}}^{\mathrm{miss}}(\mathrm{energy\ loss})$, where $E_{\mathrm{T}}^{\mathrm{miss}}(\mathrm{calo})$ is calculated from the energy deposits in calorimeter cells inside three-dimensional topological clusters [18], $E_{\mathrm{T}}^{\mathrm{miss}}(\mathrm{muon})$ is the vector sum of the muon momenta, and $E_{\mathrm{T}}^{\mathrm{miss}}(\mathrm{energy\ loss})$ is a correction term accounting for the energy lost by muons in the calorimeters. There is no direct requirement on $E_{\mathrm{T}}^{\mathrm{miss}}$ applied in this analysis but the quantity and its direction is used in several selection criteria described later.

6. Lepton isolation

Leptons from $\gamma^*/Z \to \tau\tau$ decays are typically isolated from other particles, in contrast to electrons and muons from multijet events (e.g. coming from b-hadron decays). Hence isolation requirements are applied to both the electron and muon candidates used in the four final states considered.

The first isolation variable is based on the total transverse momentum of charged particles in the inner detector in a cone of size $\Delta R = 0.4$ centered around the lepton direction, $I_{PT}^{0.4}$, divided by the transverse momentum or energy of the muon or electron candidate, respectively. A selection requiring $I_{PT}^{0.4}/p_{\mathrm{T}} < 0.06$ for the muon candidate and $I_{PT}^{0.4}/E_{\mathrm{T}} < 0.06$ for the electron candidate is used for all final states except the $\tau_\mu\tau_\mu$ final state where a looser selection, $I_{PT}^{0.4}/p_{\mathrm{T}} < 0.15$, is applied. Due to the presence of two muon candidates the multijet background is smaller in this final state, and the looser isolation requirement provides a larger signal efficiency.

A second isolation variable is based on the total transverse energy measured in the calorimeters in a cone ΔR around the lepton direction, $I_{ET}^{\Delta R}$, divided by the trans-

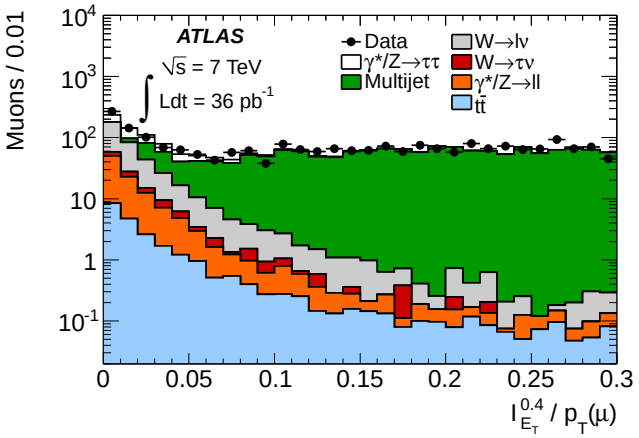

(a)

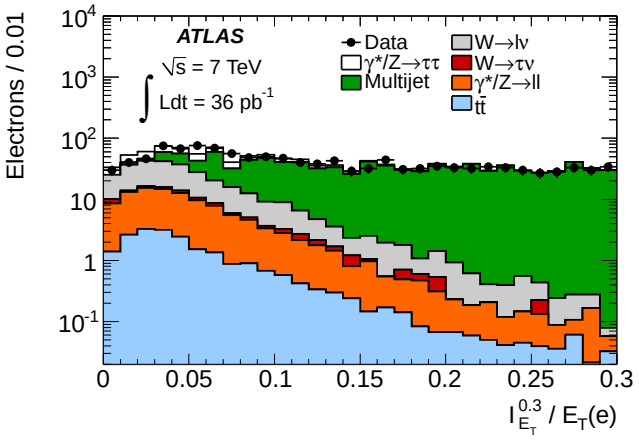

(b)

FIG. 1. Isolation variables (a) $I_{ET}^{0.4}/p_{\mathrm{T}}$ for muon and (b) $I_{ET}^{0.3}/E_{\mathrm{T}}$ for electron candidates, after selecting one hadronic τ candidate and one lepton with opposite signs in $\tau_\mu\tau_h$ and $\tau_e\tau_h$ final states respectively. The multijet background is estimated from data according to the method described in Section V; all other processes are estimated using MC simulations.

verse momentum or energy of the muon or electron candidate, respectively. For muon candidates, a cone of size $\Delta R = 0.4$ is used, and the requirement $I_{ET}^{0.4}/p_{\mathrm{T}} < 0.06$ is applied to all final states but the $\tau_\mu\tau_\mu$ final state where a looser selection, $I_{ET}^{0.4}/p_{\mathrm{T}} < 0.2$, is applied. For electron candidates, a cone of size $\Delta R = 0.3$ is used and a selection requiring $I_{ET}^{0.3}/E_{\mathrm{T}} < 0.1$ is applied in both $\tau_e\tau_h$ and $\tau_e\tau_\mu$ final states. In the reconstruction of all the isolation variables, the lepton p_{T} or E_{T} is subtracted.

The efficiencies for these isolation requirements are measured in data using $Z \to \mu\mu$ and $Z \to ee$ events and found to be $75-98\%$ for muons and $60-95\%$ for electrons, depending on the transverse momentum or energy respectively. Figure 1 shows the distribution of the $I_{ET}^{0.4}/p_{\mathrm{T}}$ variable for muon and $I_{ET}^{0.3}/E_{\mathrm{T}}$ variable for electron candidates.

B. Event selection

To select the required event topologies, the following selections are applied for the final states considered in this analysis:

- $\tau_\mu\tau_h$: at least one isolated muon candidate with $p_{\mathrm{T}} > 15$ GeV and one hadronic τ candidate with $p_{\mathrm{T}} > 20$ GeV,
- $\tau_e\tau_h$: at least one isolated "tight" electron candidate with $E_{\mathrm{T}} > 16$ GeV and one hadronic τ candidate with $p_{\mathrm{T}} > 20$ GeV,
- $\tau_e\tau_\mu$: exactly one isolated "medium" electron candidate with $E_{\mathrm{T}} > 16$ GeV and one isolated muon candidate with $p_{\mathrm{T}} > 10$ GeV,
- $\tau_\mu\tau_\mu$: exactly two isolated muon candidates with $p_{\mathrm{T}} > 10$ GeV, at least one of which should have $p_{\mathrm{T}} > 15$ GeV.

These selections are followed by a number of event-level selection criteria optimized to suppress electroweak backgrounds.

1. $\tau_\ell\tau_h$ final states

The multijet background is largely suppressed by the τ identification and lepton isolation requirements previously discussed. Events due to $W \to \ell\nu$, $W \to \tau\nu \to \ell\nu\nu\nu$, and $\gamma^*/Z \to \ell\ell$ decays can be rejected with additional event-level selection criteria.

Any event with more than one muon or electron candidate is vetoed, which strongly suppresses background from $\gamma^*/Z \to \ell\ell$ + jets events. To increase the background rejection, the selection criteria for the second lepton are relaxed with respect to those described in Section IV A: the inner detector track quality requirements are dropped for the muons, while the electrons need only pass the "medium" selection and have $E_T > 15$ GeV.

In order to suppress the W+jets background, two additional selection criteria are applied. For signal events the $E_{\mathrm{T}}^{\mathrm{miss}}$ vector is expected to fall in the azimuthal range spanned by the decay products, while in $W \to \ell\nu$ + jets events it will tend to point outside of the angle between the jet faking the τ decay products and the lepton. Hence the discriminating variable $\sum \cos\Delta\phi$ is defined as

$$\sum \cos\Delta\phi = \cos\left(\phi(\ell) - \phi(E_{\mathrm{T}}^{\mathrm{miss}})\right) + \cos\left(\phi(\tau_{\mathrm{h}}) - \phi(E_{\mathrm{T}}^{\mathrm{miss}})\right). \quad (1)$$

The variable $\sum \cos\Delta\phi$ is positive when the $E_{\mathrm{T}}^{\mathrm{miss}}$ vector points towards the direction bisecting the decay products and is negative when it points away. The distributions of $\sum \cos\Delta\phi$ are shown in Figure 2(a) and 2(b) for the $\tau_\mu\tau_h$ and $\tau_e\tau_h$ final states, respectively. The peak at zero corresponds to $\gamma^*/Z \to \tau\tau$ events where the decay products

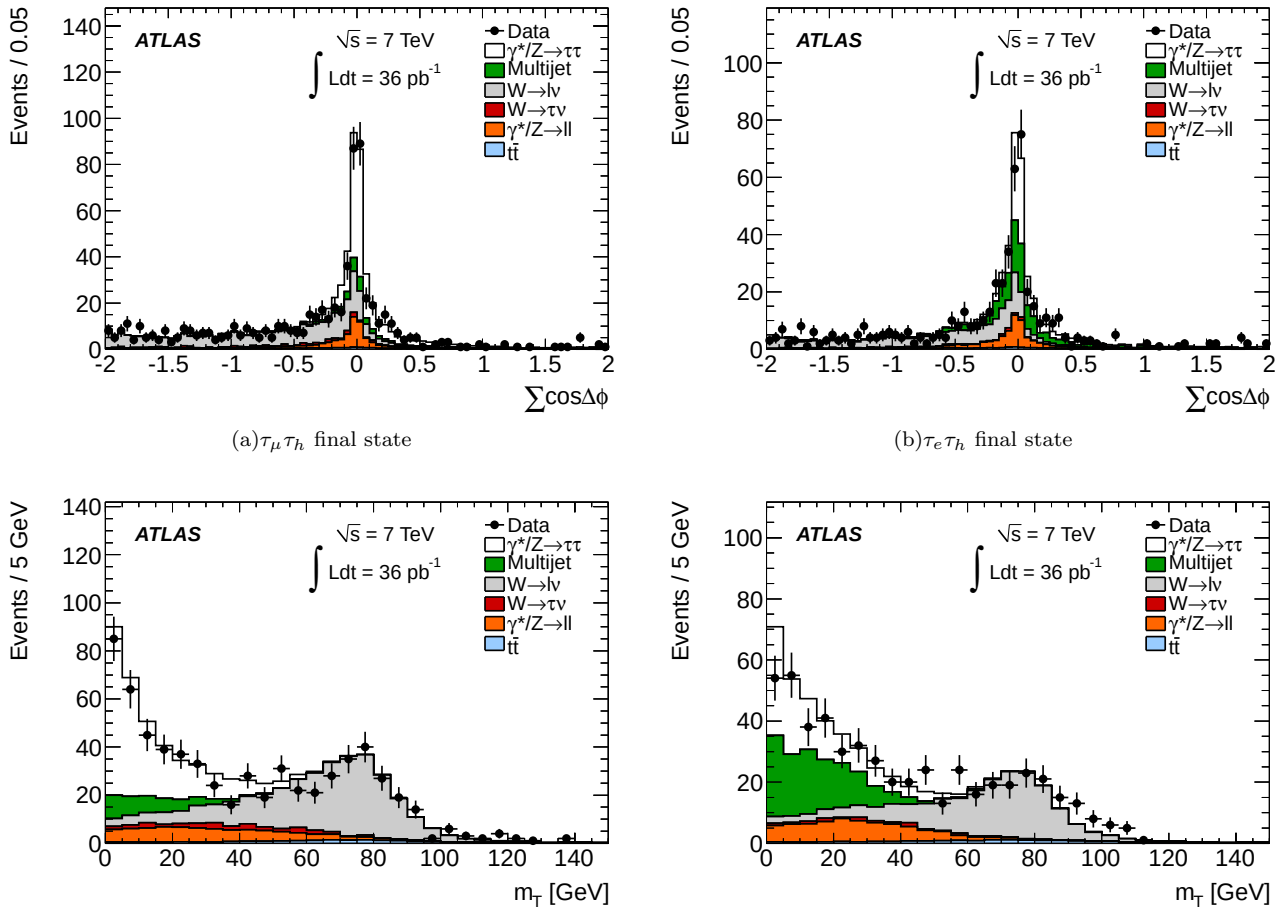

(a)$\tau_\mu\tau_h$ final state

(b)$\tau_e\tau_h$ final state

(c)$\tau_\mu\tau_h$ final state

(d)$\tau_e\tau_h$ final state

FIG. 2. The distributions of $\sum\cos\Delta\phi$ are shown for the (a) $\tau_\mu\tau_h$ and (b) $\tau_e\tau_h$ final states. The distributions of the transverse mass, $m_{\rm T}$, are shown for the (c) $\tau_\mu\tau_h$ and (d) $\tau_e\tau_h$ final states. All distributions are shown after the object selection for the given final state and after requiring exactly one muon or electron candidate. A requirement on the charge of the τ candidate to be of opposite sign to that of the lepton is also applied. The multijet background is estimated from data according to the method described in Section V; all other processes are estimated using MC simulations.

are back-to-back in the transverse plane. The $W+$jets backgrounds accumulate at negative $\sum\cos\Delta\phi$ whereas the $\gamma^*/Z\to\tau\tau$ distribution has an asymmetric tail extending into positive $\sum\cos\Delta\phi$ values, corresponding to events where the Z boson has higher $p_{\rm T}$. Events are therefore selected by requiring $\sum\cos\Delta\phi > -0.15$. Even though the resolution of the $\phi(E_{\rm T}^{\rm miss})$ direction is degraded for low values of $E_{\rm T}^{\rm miss}$, this has no adverse effect on the impact of this selection, as such events correspond to $\sum\cos\Delta\phi\sim 0$ and hence pass the selection.

To further suppress the $W+$jets background, the transverse mass, defined as

$$m_{\rm T} = \sqrt{2\,p_{\rm T}(\ell)\cdot E_{\rm T}^{\rm miss}\cdot\left(1-\cos\Delta\phi(\ell, E_{\rm T}^{\rm miss})\right)}\,, \quad (2)$$

is required to be $m_{\rm T} < 50$ GeV. Figures 2(c) and 2(d) show the distribution of m_T for the $\tau_\mu\tau_h$ and $\tau_e\tau_h$ final states, respectively.

The visible mass $m_{\rm vis}$ is defined as the invariant mass of the visible decay products of the two τ leptons. Selected events are required to have a visible mass in the range $35 < m_{\rm vis} < 75$ GeV. This window is chosen to include the bulk of the signal, while avoiding background contamination from $Z\to\ell\ell$ decays. For $Z\to\mu\mu$ events the peak is at slightly lower values than for $Z\to ee$ events, for two reasons: muons misidentified as τ candidates leave less energy in the calorimeter compared to misidentified electrons, and the proportion of events where the τ candidate arises from a misidentified jet, as opposed to a misidentified lepton, is higher in $Z\to\mu\mu$ events.

Furthermore, the chosen τ candidate is required to have exactly 1 or 3 associated tracks and a reconstructed charge of unit magnitude, characteristic of hadronic τ decays. The charge is determined as the sum of the charges of the associated tracks. Finally, the chosen τ candidate and the chosen lepton are required to have opposite charges as expected from $Z\to\tau\tau$ decays.

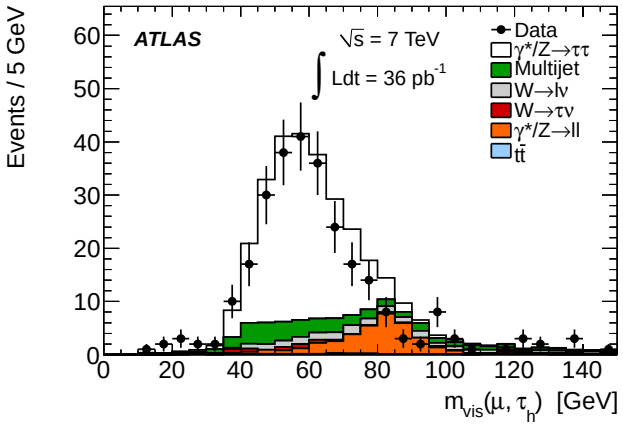

(a)$\tau_\mu\tau_h$ final state

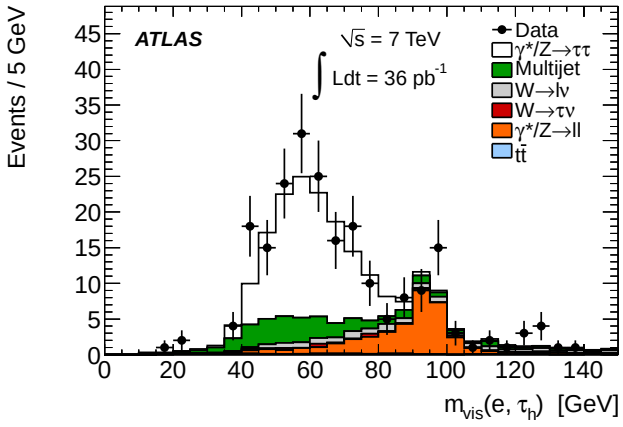

(b)$\tau_e\tau_h$ final state

FIG. 3. The distributions of the visible mass of the combination of the τ candidate and the lepton are shown for the (a) $\tau_\mu\tau_h$ and (b) $\tau_e\tau_h$ final states. These distributions are shown after the full event selection, except for the visible mass window requirement.

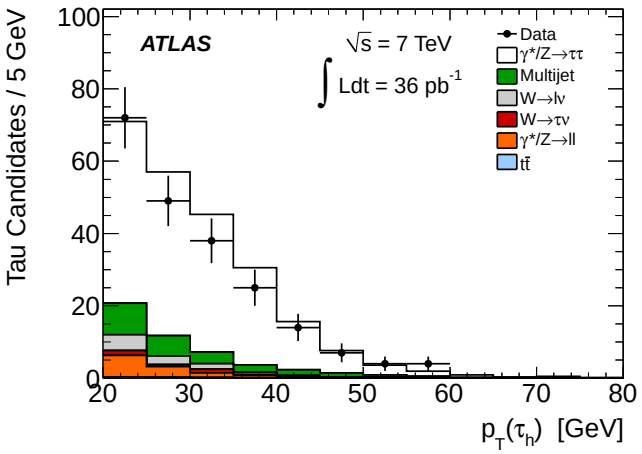

(a)$\tau_\mu\tau_h$ final state

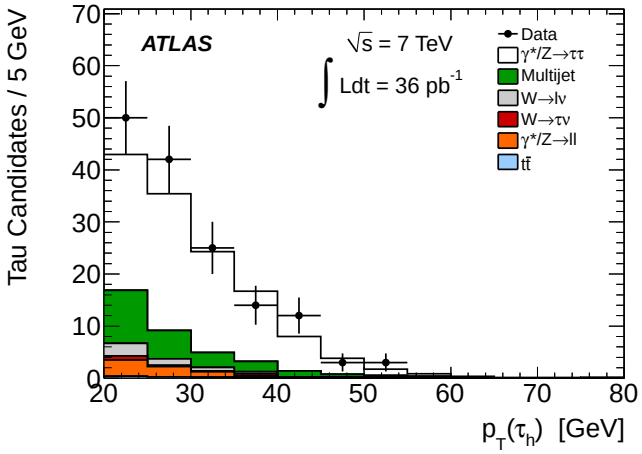

(b)$\tau_e\tau_h$ final state

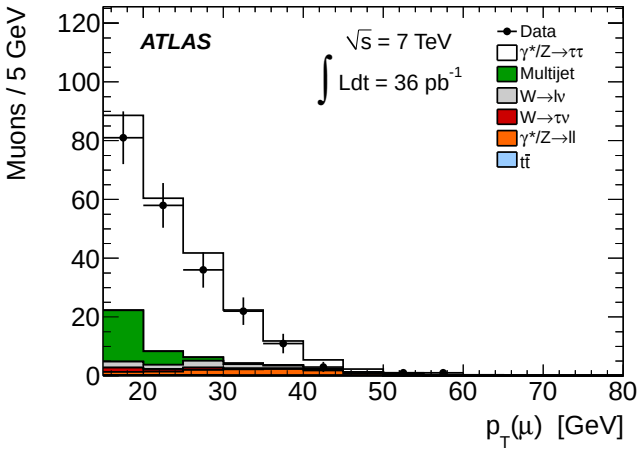

(c)$\tau_\mu\tau_h$ final state

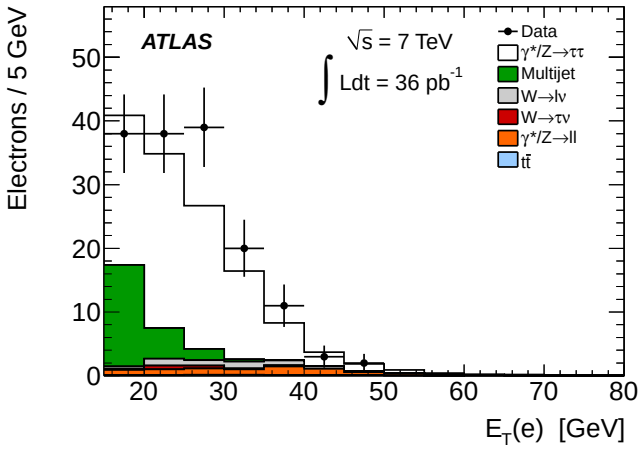

(d)$\tau_e\tau_h$ final state

FIG. 4. Distributions of the p_{T} of the τ candidate and of the muon and E_{T} of the electron, for events passing all signal selections for the $\tau_\mu\tau_h$ and $\tau_e\tau_h$ final states.

The distribution of the visible mass after the full selection except the visible mass window requirement is shown in Figure 3. The distributions of the lepton and τ candidate p_{T}, for events passing all signal selection criteria, are shown in Figure 4. The τ candidate track distribution after the full selection except the requirements on the number of associated tracks and on the magnitude of the τ charge is shown in Figure 5.

2. $\tau_e\tau_\mu$ final state

The $\tau_e\tau_\mu$ events are characterized by the presence of two oppositely charged and isolated leptons in the final state. Thus exactly one electron and one muon candidate of opposite electric charge, which pass the selections described in Section IV A, are required. For events that contain two leptons of different flavors, the contributions from $\gamma^*/Z \rightarrow ee$ and $\gamma^*/Z \rightarrow \mu\mu$ processes is small. The remaining background is therefore due to W and Z leptonic decays, where an additional real or fake lepton comes from jet fragmentation.

To reduce the $W \rightarrow e\nu$, $W \rightarrow \mu\nu$, and $t\bar{t}$ backgrounds, the requirement $\sum \cos\Delta\phi > -0.15$ is applied as in the semileptonic final states. Figure 6 shows the distribution of $\sum \cos\Delta\phi$ after the previous selection criteria.

A further requirement is made to reduce the $t\bar{t}$ background. Unlike for the signal, the topology of $t\bar{t}$ events is characterized by the presence of high-p_{T} jets and leptons, as well as large $E_{\mathrm{T}}^{\mathrm{miss}}$.

Hence the variable

$$\sum E_{\mathrm{T}} + E_{\mathrm{T}}^{\mathrm{miss}} = E_{\mathrm{T}}(e) + p_{\mathrm{T}}(\mu) + \sum_{jets} p_{\mathrm{T}} + E_{\mathrm{T}}^{\mathrm{miss}} \quad (3)$$

is defined, where the electron and muon candidates, the jets and $E_{\mathrm{T}}^{\mathrm{miss}}$ pass the selections described in Section IV A. The distribution of this variable for data and Monte Carlo after the $\sum \cos\Delta\phi$ requirement is shown in Figure 6. Requiring $\sum E_{\mathrm{T}} + E_{\mathrm{T}}^{\mathrm{miss}} < 150$ GeV rejects most of the $t\bar{t}$ background.

Finally, since $\gamma^*/Z \rightarrow \ell\ell$ events are a small background in this final state, the dilepton invariant mass is required to be within a wider range than in the semileptonic case: $25 < m_{e\mu} < 80$ GeV. Figure 7(a) shows the distribution of the visible mass. Figure 8 shows the p_{T} distributions of both leptons for events passing the full signal selection.

3. $\tau_\mu\tau_\mu$ final state

The $\tau_\mu\tau_\mu$ final state is characterized by two oppositely charged muons. Therefore only events that contain exactly two muon candidates with opposite charge that pass the selection criteria described in Section IV A are considered, with the additional requirement that the leading muon has a transverse momentum greater than 15 GeV. The signal region for this final state is defined by the two muon candidates having an invariant mass of $25 < m_{\mu\mu} < 65$ GeV.

A boosted decision tree (BDT) [21] is used to maximize the final signal efficiency and the discrimination power against the background. The BDT is trained using $Z \rightarrow \tau\tau$ Monte Carlo samples as signal and $\gamma^*/Z \rightarrow \mu\mu$ Monte Carlo samples as background. No other backgrounds are introduced in the training, in order to achieve the maximum separation between the signal and the main ($\gamma^*/Z \rightarrow \mu\mu$) background. The BDT is trained after the selection of two oppositely charged muon candidates whose invariant mass fall within the signal region. To maximize the available Monte Carlo statistics for training and testing, no isolation requirements are applied to the muon candidates.

The following input variables to the BDT training are used: the difference in azimuthal angle between the two muon candidates ($\Delta\phi(\mu_1, \mu_2)$), the difference in azimuthal angle between the leading muon candidate and the $E_{\mathrm{T}}^{\mathrm{miss}}$ vector ($\Delta\phi(\mu_1, E_{\mathrm{T}}^{\mathrm{miss}})$), the difference in the p_{T} of the two muon candidates ($p_{\mathrm{T}}(\mu_1) - p_{\mathrm{T}}(\mu_2)$), the transverse momentum of the leading muon candidate ($p_{\mathrm{T}}(\mu_1)$), and the sum of the absolute transverse impact parameters of the two muon candidates ($|d_0(\mu_1)| + |d_0(\mu_2)|$). Distributions of these variables for the events that are passed to the BDT are shown in Figure 9. Differences between data and Monte Carlo are consistent with the estimated systematic uncertainties, and the agreement is best in the regions most relevant for the signal and background separation. The sum of the muon transverse impact parameters has the highest discriminating power between the signal and the $\gamma^*/Z \rightarrow \mu\mu$ background. Figure 10 shows the distribution of the BDT output. Good agreement between data and MC is observed. Events are selected by requiring a BDT output greater than 0.07. Cutting on this value gives the best signal significance, and has an efficiency of 0.38 ± 0.02. The visible mass distribution after the full selection except the mass window requirement can be seen in Figure 7(b) and compared to the data. Figure 11 shows the distributions of the p_{T} of the two muon candidates passing the full $\tau_\mu\tau_\mu$ selection.

V. BACKGROUND ESTIMATION

In order to determine the purity of the selected $Z \rightarrow \tau\tau$ events and the $Z \rightarrow \tau\tau$ production cross section, the number of background events passing the selection criteria must be estimated. The contributions from the $\gamma^*/Z \rightarrow \ell\ell$, $t\bar{t}$ and diboson backgrounds are taken from Monte Carlo simulations, while all other backgrounds are estimated using partially or fully data-driven methods.

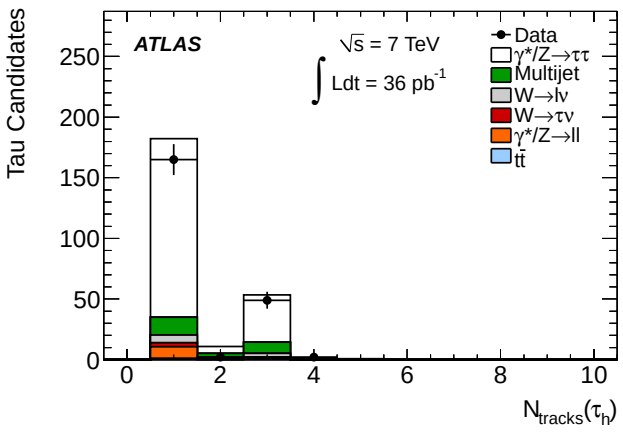

(a)$\tau_\mu\tau_h$ final state

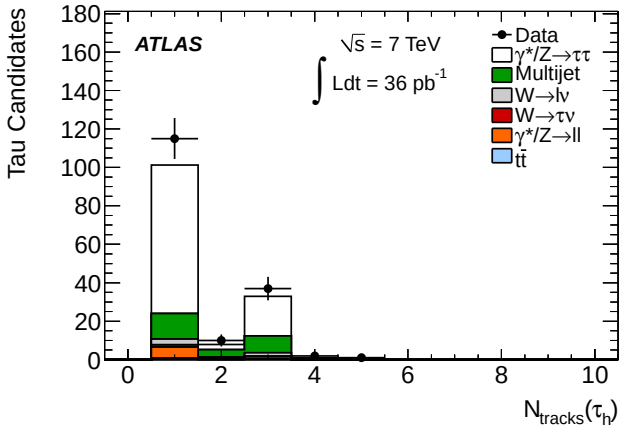

(b)$\tau_e\tau_h$ final state

FIG. 5. Distribution of the number of tracks associated to τ candidates after the full selection, including the opposite-charge requirement for the τ candidate and the lepton, except the requirement on the number of tracks and on the magnitude of the τ charge.

A. W+jets background

In the two dileptonic final states, the $W \to \ell\nu$ and $W \to \tau\nu$ backgrounds are found to be small, and their contribution is similarly obtained from simulations. In the two semileptonic final states, where these backgrounds are important, they are instead constrained with data by obtaining their normalization from a W boson-enriched control region. This normalization corrects the Monte Carlo for an overestimate of the probability for quark and gluon jets produced in association with the W to be misidentified as hadronic τ decays. The control region is defined to contain events passing all selection criteria except those (m_T, $\sum \cos\Delta\phi$) rejecting the W background. This provides a high-purity W sample. The multijet background contamination in this region is expected to be negligible, while the Monte Carlo estimate of the small $\gamma^*/Z \to \ell\ell$ and $t\bar{t}$ contribution is subtracted before calculating the normalization factor. The obtained normalization factor is 0.73 ± 0.06 (stat) for the $\tau_\mu\tau_h$ final state and 0.63 ± 0.07 (stat) for the $\tau_e\tau_h$ final state.

B. $\gamma^*/Z \to \mu\mu$ background

The most important electroweak background to the $\tau_\mu\tau_\mu$ final state comes from $\gamma^*/Z \to \mu\mu$ events. The normalization of the Monte Carlo simulation is cross-checked after the dimuon selection, for events with invariant masses between 25 GeV and 65 GeV. In this region, the $\gamma^*/Z \to \mu\mu$ process is dominant and is expected to contribute to over 94% of the selected events. The expected backgrounds arising from other electroweak processes are subtracted and the multijet contribution estimated using a data-driven method described later in this section. The number of $\gamma^*/Z \to \mu\mu$ events in the selected mass window is consistent between Monte Carlo and data within the uncertainties of ∼ 8% (to be compared with a 7% difference in rate). Therefore no correction factor is applied to the $\gamma^*/Z \to \mu\mu$ Monte Carlo prediction.

C. Multijets

The multijet background estimation is made by employing data-driven methods in all final states. In the $\tau_e\tau_\mu$, $\tau_\mu\tau_h$ and $\tau_e\tau_h$ final states, a multijet enriched control region is constructed by requiring the two candidate τ decay products to have the same sign. The ratios of events where the decay products have the opposite sign to those where they have the same sign $R_{OS/SS}$ is then measured in a separate pair of control regions where the lepton isolation requirement is inverted. Electroweak backgrounds in all three control regions are subtracted using Monte Carlo simulations. For the same-sign control regions of the semileptonic final states, the W normalization factor is recomputed using a new W control region identical to that described above, except for having the same-sign requirement applied. The reason is that the sign requirement changes the relative fraction of quark- and gluon-induced jets leading to different τ misidentification probabilities. The following values of $R_{OS/SS}$ are obtained:

1.07 ± 0.04 (stat) ± 0.04 (syst) $\tau_\mu\tau_h$ final state
1.07 ± 0.07 (stat) ± 0.07 (syst) $\tau_e\tau_h$ final state
1.55 ± 0.04 (stat) ± 0.20 (syst) $\tau_e\tau_\mu$ final state.

The $R_{OS/SS}$ ratios measured in non-isolated events are applied to the same-sign isolated events in order to estimate the multijet contribution to the signal region. The multijet background is estimated after the full selection in the two semileptonic final states, and after the dilepton selection in the $\tau_e\tau_\mu$ final state, due to limited statistics.

TABLE I. Expected number of events per process and number of events observed in data for an integrated luminosity of 36 pb^{-1}, after the full selection. The background estimates have been obtained as described in Section V. The quoted uncertainties are statistical only.

	$\tau_\mu\tau_h$	$\tau_e\tau_h$	$\tau_e\tau_\mu$	$\tau_\mu\tau_\mu$
$\gamma^*/Z \to \ell\ell$	11.1 ± 0.5	6.9 ± 0.4	1.9 ± 0.1	36 ± 1
$W \to \ell\nu$	9.3 ± 0.7	4.8 ± 0.4	0.7 ± 0.2	0.2 ± 0.1
$W \to \tau\nu$	3.6 ± 0.8	1.5 ± 0.4	< 0.2	< 0.2
$t\bar{t}$	1.3 ± 0.1	1.02 ± 0.08	0.15 ± 0.03	0.8 ± 0.1
Diboson	0.28 ± 0.02	0.18 ± 0.01	0.48 ± 0.03	0.13 ± 0.01
Multijet	24 ± 6	23 ± 6	6 ± 4	10 ± 2
$\gamma^*/Z \to \tau\tau$	186 ± 2	98 ± 1	73 ± 1	44 ± 1
Total expected events	235 ± 6	135 ± 6	82 ± 4	91 ± 3
$N_{\rm obs}$	213	151	85	90

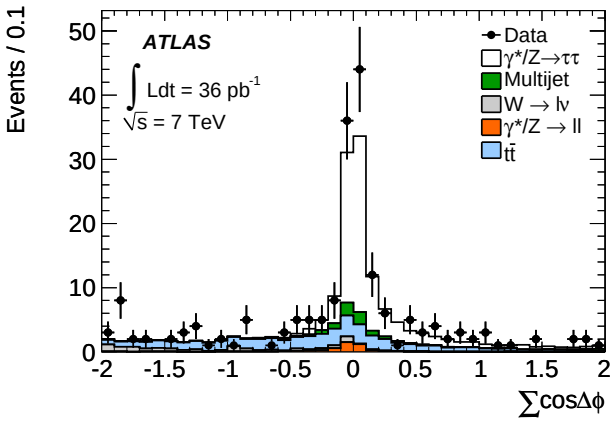

(a)$\tau_e\tau_\mu$ final state

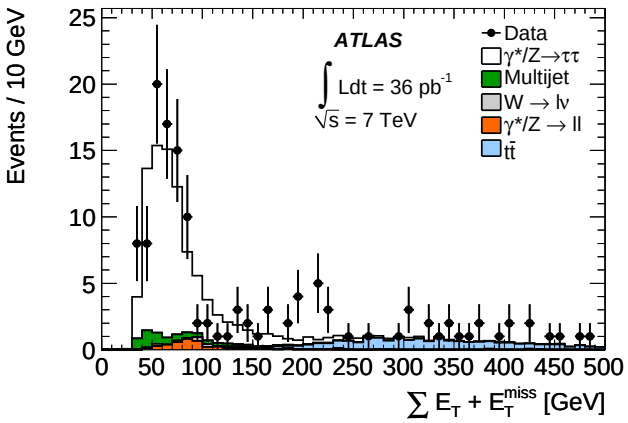

(b)$\tau_e\tau_\mu$ final state

FIG. 6. Distributions of the variables (a) $\sum\cos\Delta\phi$, after the lepton isolation selection, and (b) $\sum E_{\rm T} + E_{\rm T}^{\rm miss}$ after the $\sum\cos\Delta\phi$ selection, for the $\tau_e\tau_\mu$ final state. The multijet background is estimated from data according to the method described in Section V; all other processes are estimated using MC simulations.

The efficiency of the remaining selection criteria is obtained from the same-sign non-isolated control region.

This method assumes that the $R_{OS/SS}$ ratio is the same for non-isolated and isolated leptons. The measured variation of this ratio as a function of the isolation requirements is taken as a systematic uncertainty.

The multijet background to the $\tau_\mu\tau_\mu$ final state is estimated in a control region defined as applying the full selection, but requiring the subleading muon candidate to fail the isolation selection criteria. A scaling factor is then calculated in a separate pair of control regions, obtained by requiring that the leading muon candidate fails the isolation selection and that the subleading muon candidate either fails or passes it. This scaling factor is further corrected for the correlation between the isolation variables for the two muon candidates. The multijet background in the signal region is finally obtained from the number of events in the primary control region scaled by the corrected scaling factor.

D. Summary

Table I shows the estimated number of background events per process for all channels. The full selection described in Section IV has been applied. Also shown are the expected number of signal events, as well as the total number of events observed in data in each channel after the full selection.

VI. CROSS SECTION CALCULATION

The measurement of the cross sections is obtained using the formula

$$\sigma(Z \to \tau\tau) \times {\rm B} = \frac{N_{\rm obs} - N_{\rm bkg}}{A_Z \cdot C_Z \cdot \mathcal{L}} \qquad (4)$$

where $N_{\rm obs}$ is the number of observed events in data, $N_{\rm bkg}$ is the number of estimated background events, B

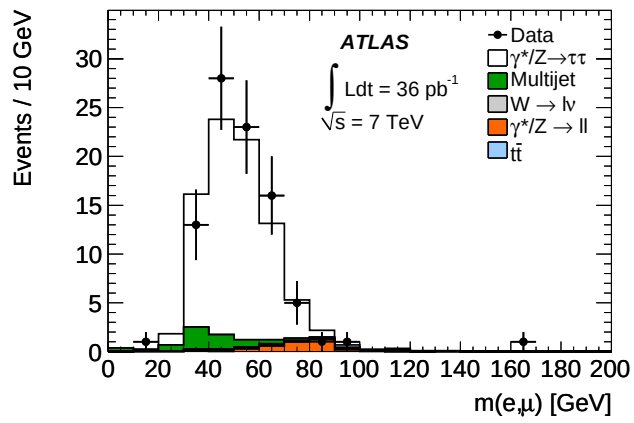

(a)$\tau_e\tau_\mu$ final state

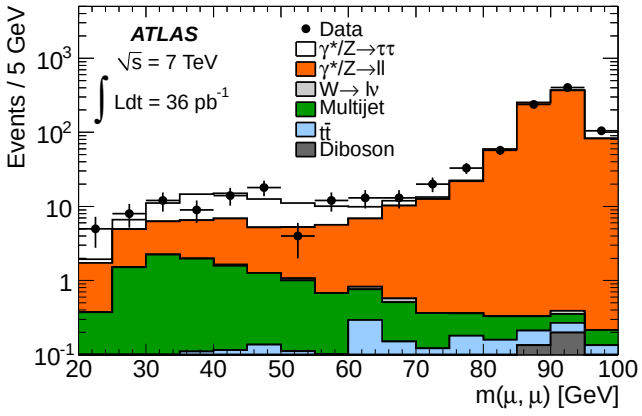

(b)$\tau_\mu\tau_\mu$ final state

FIG. 7. The distributions of the visible mass for the (a) $\tau_e\tau_\mu$ and (b) $\tau_\mu\tau_\mu$ final states, after all selections except the selection on the visible mass.

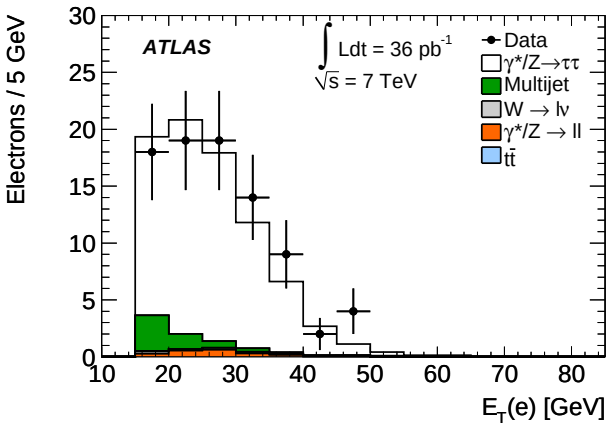

(a)$\tau_e\tau_\mu$ final state

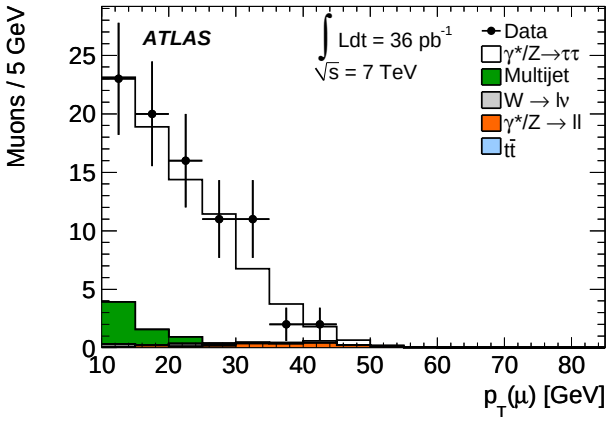

(b)$\tau_e\tau_\mu$ final state

FIG. 8. Distributions of the (a) E_{T} of the electron and (b) p_{T} of the muon, for events passing all selections for the $\tau_e\tau_\mu$ final state.

is the branching fraction for the channel considered and $\mathcal{L}$ denotes the integrated luminosity for the final state of interest. C_Z is the correction factor that accounts for the efficiency of triggering, reconstructing and identifying the $Z \to \tau\tau$ events within the fiducial regions, defined as:

$\tau_\mu\tau_h$ final state:	
Muon	$p_{\mathrm{T}} > 15$ GeV, $\lvert\eta\rvert < 2.4$
Tau	$p_{\mathrm{T}} > 20$ GeV, $\lvert\eta\rvert < 2.47$, excluding $1.37 < \lvert\eta\rvert < 1.52$
Event	$\Sigma \cos\Delta\phi > -0.15, m_{\mathrm{T}} < 50$ GeV, m_{vis} within [35, 75] GeV
$\tau_e\tau_h$ final state:	
Electron	$E_{\mathrm{T}} > 16$ GeV, $\lvert\eta\rvert < 2.47$, excluding $1.37 < \lvert\eta\rvert < 1.52$
Tau	$p_{\mathrm{T}} > 20$ GeV, $\lvert\eta\rvert < 2.47$, excluding $1.37 < \lvert\eta\rvert < 1.52$
Event	$\Sigma \cos\Delta\phi > -0.15, m_{\mathrm{T}} < 50$ GeV, m_{vis} within [35, 75] GeV
$\tau_e\tau_\mu$ final state:	
Electron	$E_{\mathrm{T}} > 16$ GeV, $\lvert\eta\rvert < 2.47$, excluding $1.37 < \lvert\eta\rvert < 1.52$
Muon	$p_{\mathrm{T}} > 10$ GeV, $\lvert\eta\rvert < 2.4$
Event	$\Sigma \cos\Delta\phi > -0.15$, m_{vis} within [25, 80] GeV
$\tau_\mu\tau_\mu$ final state:	
Leading muon	$p_{\mathrm{T}} > 15$ GeV, $\lvert\eta\rvert < 2.4$
Subleading muon	$p_{\mathrm{T}} > 10$ GeV, $\lvert\eta\rvert < 2.4$
Event	m_{vis} within [25, 65] GeV

The C_Z factor is determined as the ratio between the number of events passing the entire analysis selection after full detector simulation and the number of events in the fiducial region at generator level. The four-momenta

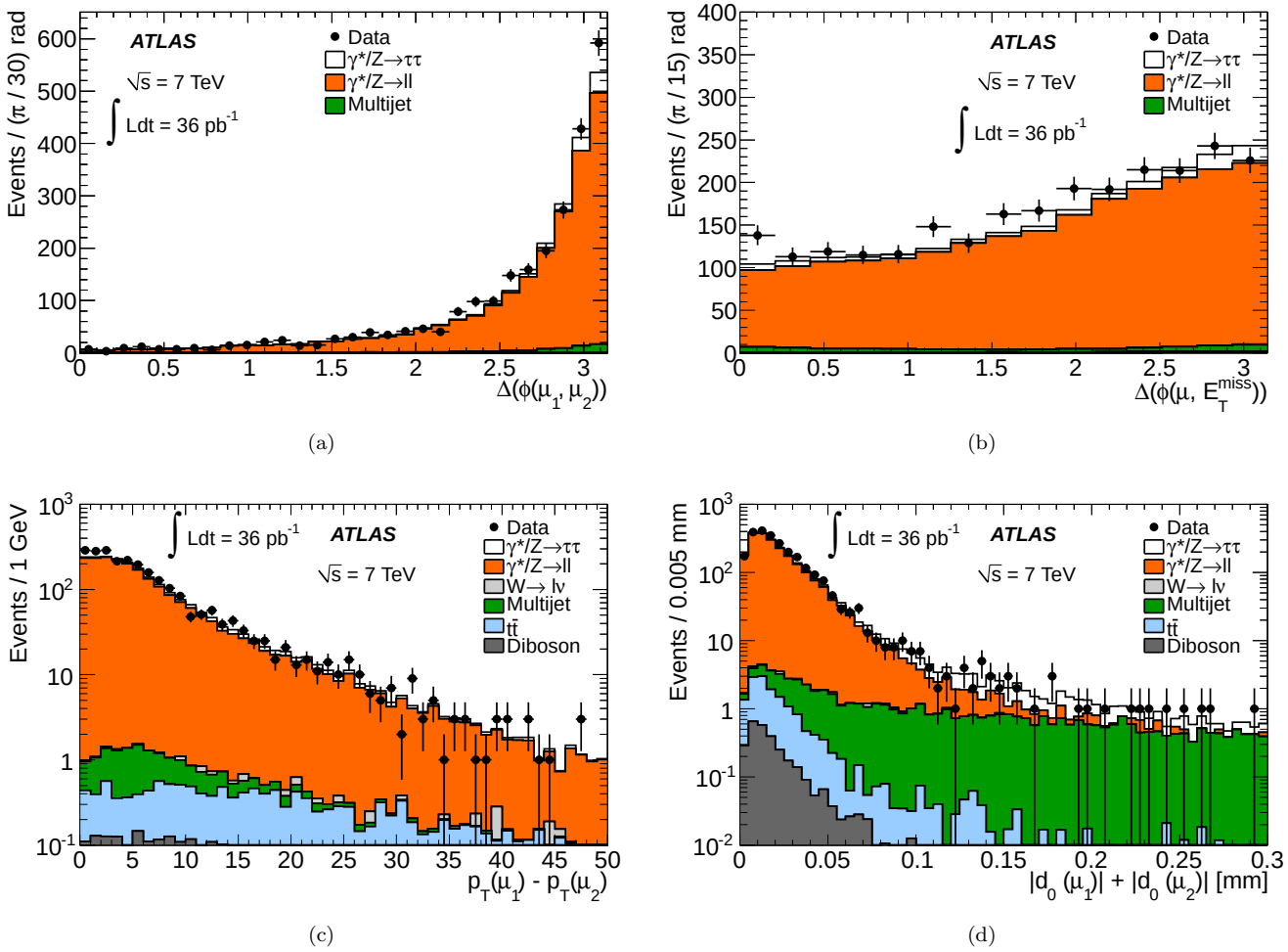

FIG. 9. Distributions of some of the input variables to the BDT used to optimize the selection of the $\tau_\mu\tau_\mu$ final state. The data are compared to signal ($\gamma^*/Z \to \tau\tau$) and $\gamma^*/Z \to \mu\mu$ Monte Carlo samples. The multijet background is estimated from data (see Section V). The observed differences are consistent with the estimated systematic uncertainties on the γ^*/Z background normalization.

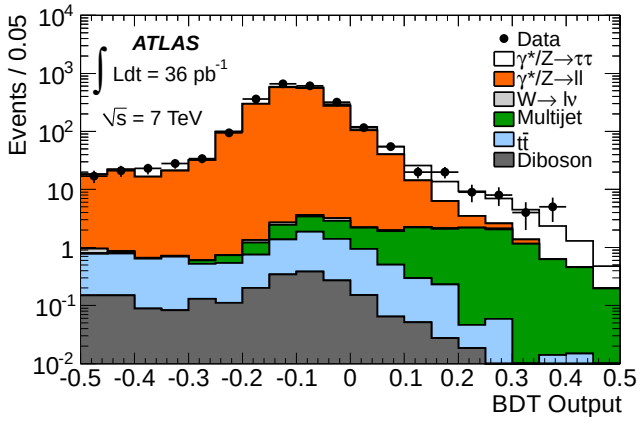

FIG. 10. The distribution of the $\tau_\mu\tau_\mu$ BDT output for the data and the expected backgrounds. Events with a BDT output greater than 0.07 are selected.

of electrons and muons are calculated including photons radiated within a cone of size $\Delta R = 0.1$. The four-momenta of the τ candidates are defined by including photons radiated by both the τ leptons and their decay products within a cone of size $\Delta R = 0.4$. By construction C_Z accounts for migrations from outside of the acceptance. The correction by the C_Z factor provides the cross section within the fiducial region of each measurement

$$\sigma^{\rm fid}(Z \to \tau\tau) \times {\rm B} = \frac{N_{\rm obs} - N_{\rm bkg}}{C_Z \cdot \mathcal{L}}, \qquad (5)$$

which is independent of the extrapolation procedure to the full phase space, and therefore is less affected by theoretical uncertainties in the modeling of the Z production.

The acceptance factor A_Z allows the extrapolation of $\sigma^{\rm fid}$ to the total cross section, defined by Eq. 4. The A_Z factor is determined from Monte Carlo as the ratio of events at generator level whose $\tau\tau$ invariant mass, before

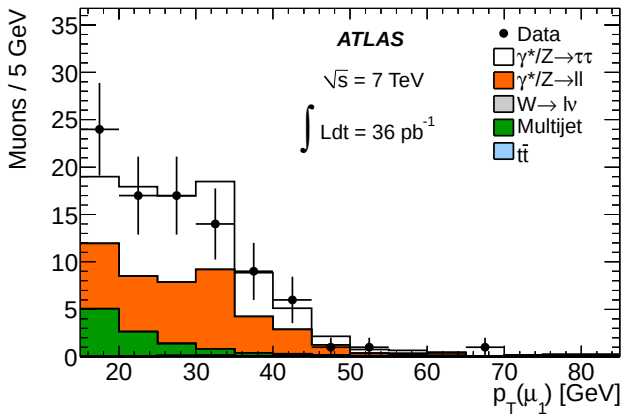

(a)

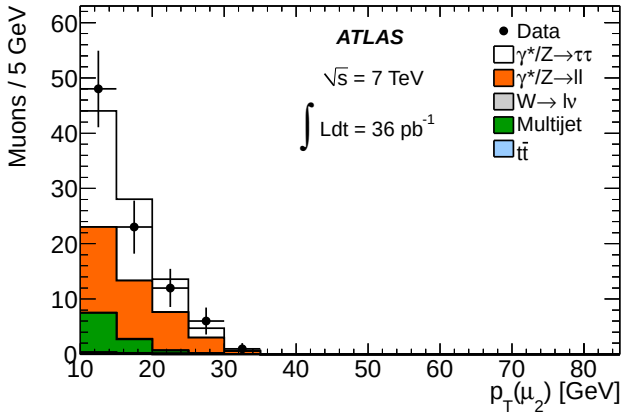

(b)

FIG. 11. Distributions of the p_{T} of (a) the leading and (b) the subleading muons, for events passing all criteria for the $\tau_\mu\tau_\mu$ final state.

final state radiation (FSR), lies within the mass window [66, 116] GeV, and the number of events at generator level that fall within the fiducial regions defined above.

The A_Z factor accounts for events that migrate from outside the invariant mass window into the fiducial selection criteria. The central values for A_Z and C_Z are determined using a PYTHIA Monte Carlo sample generated with the modified LO parton distribution functions (PDFs) MRSTLO* [22] and the corresponding ATLAS MC10 tune [7].

VII. SYSTEMATIC UNCERTAINTIES

A. Systematic uncertainty on signal and background predictions

a. Efficiency of lepton trigger, identification, and isolation As described in Sections III and IV, the efficiency of the lepton trigger, reconstruction, identification and isolation requirements are each measured separately in data, and the corresponding Monte Carlo efficiency for each step is corrected to agree with the measured values. These corrections are applied to all relevant Monte Carlo samples used for this study. Uncertainties on the corrections arise both from statistical and systematic uncertainties on the efficiency measurements.

For the electrons, when estimating the effect of these uncertainties on the signal yield and on the background predictions for each final state, the uncertainties of the individual measurements are conservatively treated as uncorrelated to each other and added in quadrature. The largest contribution to the electron efficiency uncertainty comes from the identification efficiency for low-E_{T} electrons, where the statistical uncertainty on the measurement is very large. The total electron uncertainty is estimated to be between 5-9% relative to the efficiency, depending on the selection.

For muons, the uncertainty is determined in the same way as for electrons and is estimated to be 2-4% relative to the efficiency.

b. Efficiency of hadronic τ identification The uncertainties on the hadronic τ reconstruction and identification efficiencies are evaluated by varying simulation conditions, such as the underlying event model, the amount of detector material, the hadronic shower model and the noise thresholds of the calorimeter cells in the cluster reconstruction. These contributions are added in quadrature to obtain the final systematic uncertainty in bins of p_{T} of the τ candidate and independently for the one track and three track τ candidates and for low (≤ 2) and high multiplicity of primary vertices in the event. The latter categorization is necessary due to the effects of pile-up (additional soft interactions in the same bunch crossing as the interaction that triggered the readout). In events with a large number of additional interactions the τ identification performance worsens, since the discriminating variables are diluted due to the increased activity in the tracker and calorimeters. The systematic uncertainties are estimated to be around 10% relative to the efficiency for most cases, varying between 9% and 12% with the τ candidate p_{T}, number of tracks, and number of vertices in the event [19].

c. Electron and jet misidentification as τ candidates The probability for an electron or a QCD jet to be misidentified as a hadronic τ is measured in data. The misidentification probability for electrons is determined using an identified $Z \to ee$ sample where τ identification is applied to one of the electrons. Correction factors are derived for the Monte Carlo misidentification probability for electrons, binned in η. These corrections are applied to τ candidates matched in simulation to a generator-level electron, with the uncertainty on the correction factor taken as the systematic uncertainty. The QCD jet misidentification probability is measured in $Z \to \ell\ell$+jet events. The difference to the Monte Carlo prediction for the same selection, added in quadrature with the statistical and systematic uncertainties of the measurement, is taken as the systematic uncertainty. These corrections

are applied to τ candidates not matched to a generator-level electron. The τ candidate misidentification systematic uncertainties are not applied to the W Monte Carlo samples, as these have been normalized to data to account for the QCD jet misidentification probability. Instead the uncertainty on the normalization is applied, as described later in this section.

d. Energy scale The τ energy scale uncertainty is estimated by varying the detector geometry, hadronic showering model, underlying event model as well as the noise thresholds of the calorimeter cells in the cluster reconstruction in the simulation, and comparing to the nominal results [19]. The electron energy scale is determined from data by constraining the reconstructed di-electron invariant mass to the well-known $Z \to ee$ line shape. For the central region the linearity and resolution are in addition controlled using $J/\psi \to ee$ events.

The jet energy scale uncertainty is evaluated from simulations by comparing the nominal results to Monte Carlo simulations using alternative detector configurations, alternative hadronic shower and physics models, and by comparing the relative response of jets across pseudo-rapidity between data and simulation [18]. Additionally, the calorimetric component of the $E_{\mathrm{T}}^{\mathrm{miss}}$ is sensitive to the energy scale, and this uncertainty is evaluated by propagating first the electron energy scale uncertainty into the $E_{\mathrm{T}}^{\mathrm{miss}}$ calculation and then shifting all topological clusters not associated to electrons according to their uncertainties [18].

The electron, τ and jet energy scale uncertainties, as well as the calorimetric component of the $E_{\mathrm{T}}^{\mathrm{miss}}$, are all correlated. Their effect is therefore evaluated by simultaneously shifting each up and down by one standard deviation; the jets are not considered in the semileptonic final states, while the τ candidates are not considered for the dilepton final states. The muon energy scale, and the correlated effect on the $E_{\mathrm{T}}^{\mathrm{miss}}$, is also evaluated but found to be negligible in comparison with other uncertainties.

e. Background estimation The uncertainty on the multijet background estimation arises from three separate areas. Electroweak and $t\bar{t}$ backgrounds are subtracted in the control regions and all sources of systematics on these backgrounds are taken into account. Each source of systematic error is varied up and down by one standard deviation and the effect on the final multijet background estimation is evaluated.

The second set of systematic uncertainties is related to the assumptions of the method used for the $\tau_e\tau_h$, $\tau_\mu\tau_h$, and $\tau_e\tau_\mu$ final state multijet background estimations, that the ratio of opposite-sign to same-sign events in the signal region is independent of the lepton isolation.

These systematic uncertainties are evaluated by studying the dependence of $R_{OS/SS}$ on the isolation variables selection criteria and, for the $\tau_e\tau_\mu$ channel, comparing the efficiencies of the subsequent selection criteria in the opposite and same sign regions. For the estimation of the multijet background in the $\tau_\mu\tau_\mu$ final state, the uncertainties due to the correlation between the isolation of the two muon candidates are evaluated by propagating the systematic uncertainties from the subtracted backgrounds into the calculation of the correlation factor. The third uncertainty on the multijet background estimation arises from the statistical uncertainty on the number of data events in the various control regions.

The uncertainty on the W+jets background estimation method is dominated by the statistical uncertainty on the calculation of the normalization factor in the control region, as described in Section V, and the energy scale uncertainty.

f. Muon d_0 smearing In the $\tau_\mu\tau_\mu$ final state, a smearing is applied to the transverse impact parameter of the muons with respect to the primary vertex (d_0) to match the Monte Carlo resolution with the value observed in data. The muon d_0 distribution is compared between data and Monte Carlo using a sample of $Z \to \mu\mu$ events and it is found to be well-described by a double Gaussian distribution. The 20% difference in width between data and simulation is used to define a smearing function which is applied to the d_0 of each simulated muon. The systematic uncertainty due to the smearing procedure is estimated by varying the widths and the relative weights of the two components of the impact parameter distributions applied to the Monte Carlo, within the estimated uncertainties on their measurement. An additional uncertainty is found for the $Z \to \tau\tau$ signal sample.

g. Other sources of systematic uncertainty The uncertainty on the luminosity is taken to be 3.4%, as determined in [23, 24]. A number of other sources, such as the uncertainty due to the object quality requirements on τ candidates and on jets, are also evaluated but have a small impact on the total uncertainty. The Monte Carlo is reweighted so that the distribution of the number of vertices matches that observed in data; the systematic uncertainty from the reweighting procedure amounts to a permille effect. The lepton resolution and charge misidentification are found to only have a subpercent effect on C_Z and the background predictions. Systematic uncertainties due to a few problematic calorimetric regions, affecting electron reconstruction, are also evaluated and found to a have a very small effect. The uncertainties on the theoretical cross sections by which the background Monte Carlo samples are scaled are also found to only have a very small impact on the corresponding background prediction, except for the $\tau_\mu\tau_\mu$ final state, which has a large electroweak background contamination.

B. Systematic uncertainty on the acceptance

The theoretical uncertainty on the geometric and kinematic acceptance factor A_Z is dominated by the limited knowledge of the proton PDFs and the modeling of the Z-boson production at the LHC. The uncertainty due to the choice of PDF set is evaluated by considering the max-

TABLE II. Relative statistical and systematic uncertainties in % on the total cross section measurement. The electron and muon efficiency terms include the lepton trigger, reconstruction, identification and isolation uncertainties, as described in the text. The last column indicates whether a given systematic uncertainty is treated as correlated (✓) or uncorrelated (X) among the relevant channels when combining the results, as described in Section VIII B. For the multijet background estimation method, the uncertainties in the $\tau_\mu\tau_h$, $\tau_e\tau_h$, and $\tau_e\tau_\mu$ channels are treated as correlated while the $\tau_\mu\tau_\mu$ uncertainty is treated as uncorrelated, since a different method is used, as described in Section V.

Systematic uncertainty	$\tau_\mu\tau_h$	$\tau_e\tau_h$	$\tau_e\tau_\mu$	$\tau_\mu\tau_\mu$	Correlation
Muon efficiency	3.8%	–	2.2%	8.6%	✓
Muon d_0 (shape and scale)	–	–	–	6.2%	X
Muon resolution & energy scale	0.2%	–	0.1%	1.0%	✓
Electron efficiency, resolution &					
Charge misidentification	–	9.6%	5.9%	–	✓
τ_h identification efficiency	8.6%	8.6%	–	–	✓
τ_h misidentification	1.1%	0.7%	–	–	✓
Energy scale (e/τ/jets/$E_{\mathrm{T}}^{\mathrm{miss}}$)	10%	11%	1.7%	0.1%	✓
Multijet estimate method	0.8%	2%	1.0%	1.7%	(✓)
W normalization factor	0.1%	0.2%	–	–	X
Object quality selection criteria	1.9%	1.9%	0.4%	0.4%	✓
pile-up description in simulation	0.4%	0.4%	0.5%	0.1%	✓
Theoretical cross section	0.2%	0.1%	0.3%	4.3%	✓
A_Z systematics	3%	3%	3%	4%	✓
Total Systematic uncertainty	15%	17%	7.3%	14%	
Statistical uncertainty	9.8%	12%	13%	23%	X
Luminosity	3.4%	3.4%	3.4%	3.4%	✓

imal deviation between the acceptance obtained using the default sample and the values obtained by reweighting this sample to the CTEQ6.6 and HERAPDF1.0 [25] PDF sets. The uncertainties within the PDF set are determined by using the 44 PDF error eigenvectors available [26] for the CTEQ6.6 NLO PDF set. The variations are obtained by reweighting the default sample to the relevant CTEQ6.6 error eigenvector. The uncertainties due to the modeling of W and Z production are estimated using MC@NLO interfaced with HERWIG for parton showering, with the CTEQ6.6 PDF set and ATLAS MC10 tune and a lower bound on the invariant mass of 60 GeV. Since HERWIG in association with external generators does not handle τ polarizations correctly [27], the acceptance obtained from the MC@NLO sample is corrected for this effect, which is of order 2% for the $\tau_e\tau_h$ and $\tau_\mu\tau_h$ channels, 8% for the $\tau_e\tau_\mu$ channel, and 3% for the $\tau_\mu\tau_\mu$ channel. The deviation with respect to the A_Z factor obtained using the default sample reweighted to the CTEQ6.6 PDF set central value and with an applied lower bound on the invariant mass of 60 GeV is taken as uncertainty. In the default sample the QED radiation is modeled by PHOTOS which has an accuracy of better than 0.2%, and therefore has a negligible uncertainty compared to uncertainties due to PDFs. Summing in quadrature the various contributions, total theoretical uncertainties of 3% are assigned to A_Z for both of the semileptonic and the $\tau_e\tau_\mu$ final states and of 4% for the $\tau_\mu\tau_\mu$ final state.

C. Summary of systematics

The uncertainty on the experimental acceptance C_Z is given by the effect of the uncertainties described in Section VII A on the signal Monte Carlo, after correction factors have been applied. For the total background estimation uncertainties, the correlations between the electroweak and $t\bar{t}$ background uncertainties and the multijet background uncertainty, arising from the subtraction of the former in the control regions used for the latter, are taken into account. The largest uncertainty results from the τ identification and energy scale uncertainties for the $\tau_\mu\tau_h$ and $\tau_e\tau_h$ final states. Additionally, in the $\tau_e\tau_h$ final state, the uncertainty on the electron efficiency has a large contribution. This is also the dominant uncertainty in the $\tau_e\tau_\mu$ final state. In the $\tau_\mu\tau_\mu$ final state, the uncertainty due to the muon efficiency is the dominant source, with the muon d_0 contribution being important in the background estimate contributions for that channel. The correlation between the uncertainty on C_Z and on $(N_{\mathrm{obs}} - N_{\mathrm{bkg}})$ is accounted for in obtaining the final uncertainties on the cross section measurements, which are summarized in Table II.

VIII. CROSS SECTION MEASUREMENT

A. Results by final state

The determination of the cross sections in each final state is performed by using the numbers from the previous sections, provided for reference in Table III, following the method described in Section VI. Table IV shows the cross sections measured individually in each of the four final states. Both the fiducial cross sections and the total cross sections for an invariant mass window of [66, 116] GeV are shown.

TABLE III. The components of the $Z \to \tau\tau$ cross section calculations for each final state. For $N_{\rm obs} - N_{\rm bkg}$ the first uncertainty is statistical and the second systematic. For all other values the total error is given.

	$\tau_\mu\tau_h$	$\tau_e\tau_h$
$N_{\rm obs}$	213	151
$N_{\rm obs} - N_{\rm bkg}$	$164 \pm 16 \pm 4$	$114 \pm 14 \pm 3$
A_Z	0.117 ± 0.004	0.101 ± 0.003
C_Z	0.20 ± 0.03	0.12 ± 0.02
B	0.2250 ± 0.0009	0.2313 ± 0.0009
$\mathcal{L}$	35.5 ± 1.2 pb^{-1}	35.7 ± 1.2 pb^{-1}
	$\tau_e\tau_\mu$	$\tau_\mu\tau_\mu$
$N_{\rm obs}$	85	90
$N_{\rm obs} - N_{\rm bkg}$	$76 \pm 10 \pm 1$	$43 \pm 10 \pm 3$
A_Z	0.114 ± 0.003	0.156 ± 0.006
C_Z	0.29 ± 0.02	0.27 ± 0.02
B	0.0620 ± 0.0002	0.0301 ± 0.0001
$\mathcal{L}$	35.5 ± 1.2 pb^{-1}	35.5 ± 1.2 pb^{-1}

B. Combination

The combination of the cross section measurements from the four final states is obtained by using the Best Linear Unbiased Estimate (BLUE) method, described in [28, 29]. The BLUE method determines the best estimate of the combined total cross section using a linear combination built from the individual measurements, with an estimate of σ that is unbiased and has the smallest possible variance. This is achieved by constructing a covariance matrix from the statistical and systematic uncertainties for each individual cross section measurement, while accounting for correlations between the uncertainties from each channel.

The systematic uncertainties on the individual cross sections due to different sources are assumed to either be fully correlated or fully uncorrelated. All systematic uncertainties pertaining to the efficiency and resolution of the various physics objects used in the four analyses - reconstructed electron, muon, and hadronically decaying tau candidates - are assumed to be fully correlated between final states that make use of these objects. No correlation is assumed to exist between the systematic uncertainties relating to different physics objects. Similarly, the systematic uncertainties relating to the triggers used by the analyses are taken as fully correlated for the final states using the same triggers and fully uncorrelated otherwise. The systematic uncertainty on the energy scale is conservatively taken to be fully correlated between the final states.

TABLE IV. The production cross section times branching fraction for the $Z \to \tau\tau$ process as measured in each of the four final states, and the combined result. For the fiducial cross sections the measurements include also the branching fraction of the τ to its decay products. The first error is statistical, the second systematic and the third comes from the luminosity.

Final State	Fiducial cross section (pb)
$\tau_\mu\tau_h$	$23 \pm 2 \pm 3 \pm 1$
$\tau_e\tau_h$	$27 \pm 3 \pm 5 \pm 1$
$\tau_e\tau_\mu$	$7.5 \pm 1.0 \pm 0.5 \pm 0.3$
$\tau_\mu\tau_\mu$	$4.5 \pm 1.1 \pm 0.6 \pm 0.2$
Final State	Total cross section ([66, 116] GeV) (nb)
$\tau_\mu\tau_h$	$0.86 \pm 0.08 \pm 0.12 \pm 0.03$
$\tau_e\tau_h$	$1.14 \pm 0.14 \pm 0.20 \pm 0.04$
$\tau_e\tau_\mu$	$1.06 \pm 0.14 \pm 0.08 \pm 0.04$
$\tau_\mu\tau_\mu$	$0.96 \pm 0.22 \pm 0.12 \pm 0.03$
$Z \to \tau\tau$	$0.97 \pm 0.07 \pm 0.06 \pm 0.03$

As the multijet background is estimated using the same method in the $\tau_e\tau_\mu$, $\tau_\mu\tau_h$, and $\tau_e\tau_h$ final states, the systematic uncertainty on the method is conservatively treated as fully correlated.

Finally, the systematic uncertainties on the acceptance are assumed to be completely correlated, as are the uncertainties on the luminosity and those on the theoretical cross sections used for the normalization of the Monte Carlo samples used to estimate the electroweak and $t\bar{t}$ backgrounds.

This discussion is summarized in Table II where the last column indicates whether a given source of systematic uncertainty has been treated as correlated or uncorrelated amongst the relevant channels when calculating the combined result.

Individual cross sections and their total uncertainties for the BLUE combination, as well as the weights for each of the final states in the combined cross section, together with their pulls, are also shown in Table V.

Under these assumptions, a total combined cross section of

$$\sigma(Z \to \tau\tau,\ 66 < m_{\rm inv} < 116\ \ {\rm GeV}) = 0.97 \pm 0.07\ ({\rm stat}) \pm 0.06\ ({\rm syst}) \pm 0.03\ ({\rm lumi})\ {\rm nb} \quad (6)$$

is obtained from the four final states, $\tau_\mu\tau_h$, $\tau_e\tau_h$, $\tau_e\tau_\mu$, and $\tau_\mu\tau_\mu$.

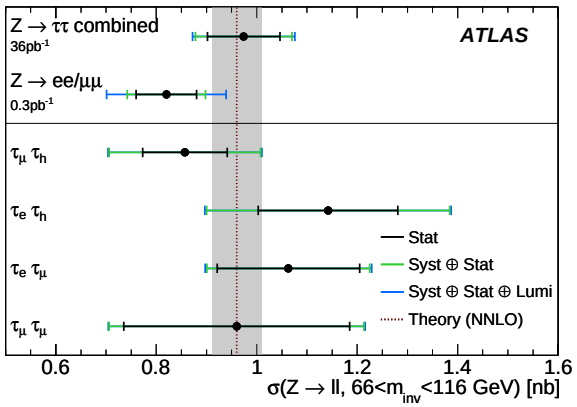

FIG. 12. The individual cross section measurements by final state, and the combined result. The $Z \to \ell\ell$ combined cross section measured by ATLAS in the $Z \to \mu\mu$ and $Z \to ee$ final states is also shown for comparison. The gray band indicates the uncertainty on the NNLO cross section prediction.

A comparison of the individual cross sections with the combined result is shown in Figure 12, along with the combined $Z \to \ell\ell$ cross section measured in the $Z \to \mu\mu$ and $Z \to ee$ final states by ATLAS [15]. The theoretical expectation of 0.96 ± 0.05 nb for an invariant mass window of $[66, 116]$ GeV is also shown. The obtained result is compatible with the $Z \to \tau\tau$ cross section in four final states published recently by the CMS Collaboration [5], $1.00 \pm 0.05\ ({\rm stat}) \pm 0.08\ ({\rm syst}) \pm 0.04\ ({\rm lumi})$ nb, in a mass window of $[60, 120]$ GeV.

TABLE V. Individual cross sections and their total uncertainties used in the BLUE combination, the weights for each of the final states in the combined cross section, and their pulls. The pull here is defined as the difference between the individual and combined cross sections divided by the uncertainty on this difference. The uncertainty on the difference between the measured and combined cross section values includes the uncertainties on the cross section both before and after the combination, taking all correlations into account.

	$\tau_\mu\tau_h$	$\tau_e\tau_h$	$\tau_e\tau_\mu$	$\tau_\mu\tau_\mu$
$\sigma_{Z\to\tau\tau}$ (nb)	0.86	1.14	1.06	0.96
Total unc. (nb)	0.15	0.24	0.17	0.25
Weight	39.4%	7.9%	39.0%	13.7%
Pull	1.02	-0.76	-0.68	0.06

IX. SUMMARY

A measurement of the $Z \to \tau\tau$ cross section in proton-proton collisions at $\sqrt{s} = 7$ TeV using the ATLAS detector is presented. Cross sections are measured in four final states, $\tau_\mu\tau_h$, $\tau_e\tau_h$, $\tau_e\tau_\mu$, and $\tau_\mu\tau_\mu$ within the invariant mass range [66, 116] GeV. The combined measurement is also reported. A total combined cross section of $\sigma = 0.97 \pm 0.07\ ({\rm stat}) \pm 0.06\ ({\rm syst}) \pm 0.03\ ({\rm lumi})$ nb is measured, which is in good agreement with the theoretical expectation and with other measurements.

ACKNOWLEDGMENTS

We thank CERN for the very successful operation of the LHC, as well as the support staff from our institutions without whom ATLAS could not be operated efficiently.

We acknowledge the support of ANPCyT, Argentina; YerPhI, Armenia; ARC, Australia; BMWF, Austria; ANAS, Azerbaijan; SSTC, Belarus; CNPq and FAPESP, Brazil; NSERC, NRC and CFI, Canada; CERN; CONICYT, Chile; CAS, MOST and NSFC, China; COLCIENCIAS, Colombia; MSMT CR, MPO CR and VSC CR, Czech Republic; DNRF, DNSRC and Lundbeck Foundation, Denmark; ARTEMIS, European Union; IN2P3-CNRS, CEA-DSM/IRFU, France; GNAS, Georgia; BMBF, DFG, HGF, MPG and AvH Foundation, Germany; GSRT, Greece; ISF, MINERVA, GIF, DIP and Benoziyo Center, Israel; INFN, Italy; MEXT and JSPS, Japan; CNRST, Morocco; FOM and NWO, Netherlands; RCN, Norway; MNiSW, Poland; GRICES and FCT, Portugal; MERYS (MECTS), Romania; MES of Russia and ROSATOM, Russian Federation; JINR; MSTD, Serbia; MSSR, Slovakia; ARRS and MVZT, Slovenia; DST/NRF, South Africa; MICINN, Spain; SRC and Wallenberg Foundation, Sweden; SER, SNSF and Cantons of Bern and Geneva, Switzerland; NSC, Taiwan; TAEK, Turkey; STFC, the Royal Society and Leverhulme Trust, United Kingdom; DOE and NSF, United States of America.

The crucial computing support from all WLCG partners is acknowledged gratefully, in particular from CERN and the ATLAS Tier-1 facilities at TRIUMF (Canada), NDGF (Denmark, Norway, Sweden), CC-IN2P3 (France), KIT/GridKA (Germany), INFN-CNAF (Italy), NL-T1 (Netherlands), PIC (Spain), ASGC (Taiwan), RAL (UK) and BNL (USA) and in the Tier-2 facilities worldwide.

[1] The ATLAS Collaboration, JINST **3**, S08003 (2008).
[2] K. Nakamura *et al.* (Particle Data Group), J. Phys. **G37**, 075021 (2010).
[3] The D0 Collaboration, Phys. Lett. **B670**, 292 (2009).
[4] The CDF Collaboration, Phys. Rev. **D75**, 092004 (2007).
[5] The CMS Collaboration, JHEP **08**, 117 (2011).
[6] The ATLAS Collaboration, arXiv:1110.1530v1 [hep-ex].
[7] The ATLAS Collaboration, ATLAS-CONF-2010-031, `http://cdsweb.cern.ch/record/1337781` (2010).
[8] S. Agostinelli *et al.* (GEANT4), Nucl. Instrum. Meth. **A506**, 250 (2003); The ATLAS Collaboration, Eur. Phys. J. **C70**, 823 (2010).
[9] T. Sjostrand, S. Mrenna, and P. Skands, JHEP **05**, 026 (2006).
[10] K. Melnikov and F. Petriello, Phys. Rev. **D74**, 114017 (2006); R. Gavin, Y. Li, F. Petriello et al., arXiv:1011.3540 [hep-ph]; S. Catani, L. Cieri, G. Ferrera, D. de Florian, and M. Grazzini, Phys. Rev. Lett. **103**, 082001 (2009).
[11] S. Frixione and B. Webber, JHEP **0206**, 029 (2002).
[12] G. Corcella *et al.*, JHEP **0101**, 010 (2001).
[13] S. Jadach, Z. Was, R. Decker, and J. H. Kühn, Comput. Phys. Commun. **76**, 361 (1993).
[14] P. Golonka and Z. Was, Eur. Phys. J. **C45**, 97 (2006).
[15] The ATLAS Collaboration, JHEP **12**, 060 (2010).
[16] The ATLAS Collaboration, ATLAS-CONF-2011-063, `http://cdsweb.cern.ch/record/1345743` (2011).
[17] M. Cacciari and G. P. Salam, Phys. Lett. **B641**, 57 (2006); M. Cacciari, G. P. Salam, and G. Soyez, "FastJet," http://fastjet.fr.
[18] The ATLAS Collaboration, Eur. Phys. J. **C71**, 1512 (2011).
[19] The ATLAS Collaboration, ATLAS-CONF-2011-077, `http://cdsweb.cern.ch/record/1353226` (2011).
[20] The ATLAS Collaboration, ATLAS-CONF-2011-113, `http://cdsweb.cern.ch/record/1375550` (2011).
[21] A. Hoecker *et al.*, PoS ACAT:040,2007, CERN-OPEN-2007-007 (2009), arXiv:physics/0703039v5.
[22] A. Sherstnev and R. S. Thorne, Eur. Phys. J. **C55**, 553 (2008).
[23] The ATLAS Collaboration, ATLAS-CONF-2011-011, `http://cdsweb.cern.ch/record/1334563` (2011).
[24] The ATLAS Collaboration, Eur. Phys. J. **C71**, 1630 (2011).
[25] The H1 and ZEUS Collaborations, JHEP **01**, 109 (2010).
[26] P. M. Nadolsky *et al.*, Phys. Rev. **D78**, 013004 (2008).
[27] D. Grellscheid and P. Richardson, arXiv:0710.1951v1.
[28] L. Lyons, D. Gibaut, and P. Clifford, Nucl. Instrum. Meth. **A270**, 110 (1988).
[29] A. Valassi, Nucl. Instrum. Meth. **A500**, 391 (2003).

The ATLAS Collaboration

G. Aad[48], B. Abbott[111], J. Abdallah[11], A.A. Abdelalim[49], A. Abdesselam[118], O. Abdinov[10], B. Abi[112], M. Abolins[88], H. Abramowicz[153], H. Abreu[115], E. Acerbi[89a,89b], B.S. Acharya[164a,164b], D.L. Adams[24], T.N. Addy[56], J. Adelman[175], M. Aderholz[99], S. Adomeit[98], P. Adragna[75], T. Adye[129], S. Aefsky[22], J.A. Aguilar-Saavedra[124b,a], M. Aharrouche[81], S.P. Ahlen[21], F. Ahles[48], A. Ahmad[148], M. Ahsan[40], G. Aielli[133a,133b], T. Akdogan[18a], T.P.A. Åkesson[79], G. Akimoto[155], A.V. Akimov [94], A. Akiyama[67], M.S. Alam[1], M.A. Alam[76], J. Albert[169], S. Albrand[55], M. Aleksa[29], I.N. Aleksandrov[65], F. Alessandria[89a], C. Alexa[25a], G. Alexander[153], G. Alexandre[49], T. Alexopoulos[9], M. Alhroob[20], M. Aliev[15], G. Alimonti[89a], J. Alison[120], M. Aliyev[10], P.P. Allport[73], S.E. Allwood-Spiers[53], J. Almond[82], A. Aloisio[102a,102b], R. Alon[171], A. Alonso[79], M.G. Alviggi[102a,102b], K. Amako[66], P. Amaral[29], C. Amelung[22], V.V. Ammosov[128], A. Amorim[124a,b], G. Amorós[167], N. Amram[153], C. Anastopoulos[29], N. Andari[115], T. Andeen[34], C.F. Anders[20], K.J. Anderson[30], A. Andreazza[89a,89b], V. Andrei[58a], M-L. Andrieux[55], X.S. Anduaga[70], A. Angerami[34], F. Anghinolfi[29], N. Anjos[124a], A. Annovi[47], A. Antonaki[8], M. Antonelli[47], A. Antonov[96], J. Antos[144b], F. Anulli[132a], S. Aoun[83], L. Aperio Bella[4], R. Apolle[118,c], G. Arabidze[88], I. Aracena[143], Y. Arai[66], A.T.H. Arce[44], J.P. Archambault[28], S. Arfaoui[29,d], J-F. Arguin[14], E. Arik[18a,*], M. Arik[18a], A.J. Armbruster[87], O. Arnaez[81], C. Arnault[115], A. Artamonov[95], G. Artoni[132a,132b], D. Arutinov[20], S. Asai[155], R. Asfandiyarov[172], S. Ask[27], B. Åsman[146a,146b], L. Asquith[5], K. Assamagan[24], A. Astbury[169], A. Astvatsatourov[52], G. Atoian[175], B. Aubert[4], B. Auerbach[175], E. Auge[115], K. Augsten[127], M. Aurousseau[145a], N. Austin[73], G. Avolio[163], R. Avramidou[9], D. Axen[168], C. Ay[54], G. Azuelos[93,e], Y. Azuma[155], M.A. Baak[29], G. Baccaglioni[89a], C. Bacci[134a,134b], A.M. Bach[14], H. Bachacou[136], K. Bachas[29], G. Bachy[29], M. Backes[49], M. Backhaus[20], E. Badescu[25a], P. Bagnaia[132a,132b], S. Bahinipati[2], Y. Bai[32a], D.C. Bailey[158], T. Bain[158], J.T. Baines[129], O.K. Baker[175], M.D. Baker[24], S. Baker[77], F. Baltasar Dos Santos Pedrosa[29], E. Banas[38], P. Banerjee[93], Sw. Banerjee[172], D. Banfi[29], A. Bangert[137], V. Bansal[169], H.S. Bansil[17], L. Barak[171], S.P. Baranov[94], A. Barashkou[65], A. Barbaro Galtieri[14], T. Barber[27], E.L. Barberio[86], D. Barberis[50a,50b], M. Barbero[20], D.Y. Bardin[65], T. Barillari[99], M. Barisonzi[174], T. Barklow[143], N. Barlow[27], B.M. Barnett[129], R.M. Barnett[14], A. Baroncelli[134a], G. Barone[49], A.J. Barr[118], F. Barreiro[80], J. Barreiro Guimarães da Costa[57], P. Barrillon[115], R. Bartoldus[143], A.E. Barton[71], D. Bartsch[20], V. Bartsch[149], R.L. Bates[53], L. Batkova[144a], J.R. Batley[27], A. Battaglia[16], M. Battistin[29], G. Battistoni[89a], F. Bauer[136], H.S. Bawa[143,f], B. Beare[158], T. Beau[78], P.H. Beauchemin[118], R. Beccherle[50a], P. Bechtle[41], H.P. Beck[16], M. Beckingham[48], K.H. Becks[174], A.J. Beddall[18c], A. Beddall[18c], S. Bedikian[175], V.A. Bednyakov[65], C.P. Bee[83], M. Begel[24], S. Behar Harpaz[152], P.K. Behera[63], M. Beimforde[99], C. Belanger-Champagne[85], P.J. Bell[49], W.H. Bell[49], G. Bella[153], L. Bellagamba[19a], F. Bellina[29], M. Bellomo[119a], A. Belloni[57], O. Beloborodova[107], K. Belotskiy[96], O. Beltramello[29], S. Ben Ami[152], O. Benary[153], D. Benchekroun[135a], C. Benchouk[83], M. Bendel[81], B.H. Benedict[163], N. Benekos[165], Y. Benhammou[153], D.P. Benjamin[44], M. Benoit[115], J.R. Bensinger[22], K. Benslama[130], S. Bentvelsen[105], D. Berge[29], E. Bergeaas Kuutmann[41], N. Berger[4], F. Berghaus[169], E. Berglund[49], J. Beringer[14], K. Bernardet[83], P. Bernat[77], R. Bernhard[48], C. Bernius[24], T. Berry[76], A. Bertin[19a,19b], F. Bertinelli[29], F. Bertolucci[122a,122b], M.I. Besana[89a,89b], N. Besson[136], S. Bethke[99], W. Bhimji[45], R.M. Bianchi[29], M. Bianco[72a,72b], O. Biebel[98], S.P. Bieniek[77], J. Biesiada[14], M. Biglietti[134a,134b], H. Bilokon[47], M. Bindi[19a,19b], S. Binet[115], A. Bingul[18c], C. Bini[132a,132b], C. Biscarat[177], U. Bitenc[48], K.M. Black[21], R.E. Blair[5], J.-B. Blanchard[115], G. Blanchot[29], T. Blazek[144a], C. Blocker[22], J. Blocki[38], A. Blondel[49], W. Blum[81], U. Blumenschein[54], G.J. Bobbink[105], V.B. Bobrovnikov[107], S.S. Bocchetta[79], A. Bocci[44], C.R. Boddy[118], M. Boehler[41], J. Boek[174], N. Boelaert[35], S. Böser[77], J.A. Bogaerts[29], A. Bogdanchikov[107], A. Bogouch[90,*], C. Bohm[146a], V. Boisvert[76], T. Bold[163,g], V. Boldea[25a], N.M. Bolnet[136], M. Bona[75], V.G. Bondarenko[96], M. Boonekamp[136], G. Boorman[76], C.N. Booth[139], S. Bordoni[78], C. Borer[16], A. Borisov[128], G. Borissov[71], I. Borjanovic[12a], S. Borroni[132a,132b], K. Bos[105], D. Boscherini[19a], M. Bosman[11], H. Boterenbrood[105], D. Botterill[129], J. Bouchami[93], J. Boudreau[123], E.V. Bouhova-Thacker[71], C. Boulahouache[123], C. Bourdarios[115], N. Bousson[83], A. Boveia[30], J. Boyd[29], I.R. Boyko[65], N.I. Bozhko[128], I. Bozovic-Jelisavcic[12b], J. Bracinik[17], A. Braem[29], P. Branchini[134a], G.W. Brandenburg[57], A. Brandt[7], G. Brandt[15], O. Brandt[54], U. Bratzler[156], B. Brau[84], J.E. Brau[114], H.M. Braun[174], B. Brelier[158], J. Bremer[29], R. Brenner[166], S. Bressler[152], D. Breton[115], D. Britton[53], F.M. Brochu[27], I. Brock[20], R. Brock[88], T.J. Brodbeck[71], E. Brodet[153], F. Broggi[89a], C. Bromberg[88], G. Brooijmans[34], W.K. Brooks[31b], G. Brown[82], H. Brown[7], P.A. Bruckman de Renstrom[38], D. Bruncko[144b], R. Bruneliere[48], S. Brunet[61], A. Bruni[19a], G. Bruni[19a], M. Bruschi[19a], T. Buanes[13], F. Bucci[49], J. Buchanan[118], N.J. Buchanan[2], P. Buchholz[141], R.M. Buckingham[118], A.G. Buckley[45], S.I. Buda[25a], I.A. Budagov[65], B. Budick[108], V. Büscher[81], L. Bugge[117], D. Buira-Clark[118], O. Bulekov[96], M. Bunse[42], T. Buran[117], H. Burckhart[29], S. Burdin[73], T. Burgess[13], S. Burke[129], E. Busato[33], P. Bussey[53], C.P. Buszello[166], F. Butin[29], B. Butler[143], J.M. Butler[21], C.M. Buttar[53], J.M. Butterworth[77], W. Buttinger[27], T. Byatt[77], S. Cabrera Urbán[167], D. Caforio[19a,19b], O. Cakir[3a], P. Calafiura[14], G. Calderini[78], P. Calfayan[98], R. Calkins[106], L.P. Caloba[23a], R. Caloi[132a,132b], D. Calvet[33], S. Calvet[33], R. Camacho Toro[33], P. Camarri[133a,133b], M. Cambiaghi[119a,119b], D. Cameron[117], S. Campana[29], M. Campanelli[77], V. Canale[102a,102b], F. Canelli[30], A. Canepa[159a], J. Cantero[80],

L. Capasso[102a,102b], M.D.M. Capeans Garrido[29], I. Caprini[25a], M. Caprini[25a], D. Capriotti[99], M. Capua[36a,36b], R. Caputo[148], C. Caramarcu[25a], R. Cardarelli[133a], T. Carli[29], G. Carlino[102a], L. Carminati[89a,89b], B. Caron[159a], S. Caron[48], G.D. Carrillo Montoya[172], A.A. Carter[75], J.R. Carter[27], J. Carvalho[124a,h], D. Casadei[108], M.P. Casado[11], M. Cascella[122a,122b], C. Caso[50a,50b,*], A.M. Castaneda Hernandez[172], E. Castaneda-Miranda[172], V. Castillo Gimenez[167], N.F. Castro[124a], G. Cataldi[72a], F. Cataneo[29], A. Catinaccio[29], J.R. Catmore[71], A. Cattai[29], G. Cattani[133a,133b], S. Caughron[88], D. Cauz[164a,164c], P. Cavalleri[78], D. Cavalli[89a], M. Cavalli-Sforza[11], V. Cavasinni[122a,122b], F. Ceradini[134a,134b], A.S. Cerqueira[23a], A. Cerri[29], L. Cerrito[75], F. Cerutti[47], S.A. Cetin[18b], F. Cevenini[102a,102b], A. Chafaq[135a], D. Chakraborty[106], K. Chan[2], B. Chapleau[85], J.D. Chapman[27], J.W. Chapman[87], E. Chareyre[78], D.G. Charlton[17], V. Chavda[82], C.A. Chavez Barajas[29], S. Cheatham[85], S. Chekanov[5], S.V. Chekulaev[159a], G.A. Chelkov[65], M.A. Chelstowska[104], C. Chen[64], H. Chen[24], S. Chen[32c], T. Chen[32c], X. Chen[172], S. Cheng[32a], A. Cheplakov[65], V.F. Chepurnov[65], R. Cherkaoui El Moursli[135e], V. Chernyatin[24], E. Cheu[6], S.L. Cheung[158], L. Chevalier[136], G. Chiefari[102a,102b], L. Chikovani[51], J.T. Childers[58a], A. Chilingarov[71], G. Chiodini[72a], M.V. Chizhov[65], G. Choudalakis[30], S. Chouridou[137], I.A. Christidi[77], A. Christov[48], D. Chromek-Burckhart[29], M.L. Chu[151], J. Chudoba[125], G. Ciapetti[132a,132b], K. Ciba[37], A.K. Ciftci[3a], R. Ciftci[3a], D. Cinca[33], V. Cindro[74], M.D. Ciobotaru[163], C. Ciocca[19a,19b], A. Ciocio[14], M. Cirilli[87], M. Ciubancan[25a], A. Clark[49], P.J. Clark[45], W. Cleland[123], J.C. Clemens[83], B. Clement[55], C. Clement[146a,146b], R.W. Clifft[129], Y. Coadou[83], M. Cobal[164a,164c], A. Coccaro[50a,50b], J. Cochran[64], P. Coe[118], J.G. Cogan[143], J. Coggeshall[165], E. Cogneras[177], C.D. Cojocaru[28], J. Colas[4], A.P. Colijn[105], C. Collard[115], N.J. Collins[17], C. Collins-Tooth[53], J. Collot[55], G. Colon[84], P. Conde Muiño[124a], E. Coniavitis[118], M.C. Conidi[11], M. Consonni[104], S.M. Consonni[89a,89b], V. Consorti[48], S. Constantinescu[25a], C. Conta[119a,119b], F. Conventi[102a,i], J. Cook[29], M. Cooke[14], B.D. Cooper[77], A.M. Cooper-Sarkar[118], N.J. Cooper-Smith[76], K. Copic[34], T. Cornelissen[50a,50b], M. Corradi[19a], F. Corriveau[85,j], A. Cortes-Gonzalez[165], G. Cortiana[99], G. Costa[89a], M.J. Costa[167], D. Costanzo[139], T. Costin[30], D. Côté[29], R. Coura Torres[23a], L. Courneyea[169], G. Cowan[76], C. Cowden[27], B.E. Cox[82], K. Cranmer[108], F. Crescioli[122a,122b], M. Cristinziani[20], G. Crosetti[36a,36b], R. Crupi[72a,72b], S. Crépé-Renaudin[55], C.-M. Cuciuc[25a], C. Cuenca Almenar[175], T. Cuhadar Donszelmann[139], M. Curatolo[47], C.J. Curtis[17], P. Cwetanski[61], H. Czirr[141], Z. Czyczula[117], S. D'Auria[53], M. D'Onofrio[73], A. D'Orazio[132a,132b], P.V.M. Da Silva[23a], C. Da Via[82], W. Dabrowski[37], T. Dai[87], C. Dallapiccola[84], M. Dam[35], M. Dameri[50a,50b], D.S. Damiani[137], H.O. Danielsson[29], D. Dannheim[99], V. Dao[49], G. Darbo[50a], G.L. Darlea[25b], C. Daum[105], J.P. Dauvergne [29], W. Davey[86], T. Davidek[126], N. Davidson[86], R. Davidson[71], E. Davies[118,c], M. Davies[93], A.R. Davison[77], Y. Davygora[58a], E. Dawe[142], I. Dawson[139], J.W. Dawson[5,*], R.K. Daya[39], K. De[7], R. de Asmundis[102a], S. De Castro[19a,19b], P.E. De Castro Faria Salgado[24], S. De Cecco[78], J. de Graat[98], N. De Groot[104], P. de Jong[105], C. De La Taille[115], H. De la Torre[80], B. De Lotto[164a,164c], L. De Mora[71], L. De Nooij[105], M. De Oliveira Branco[29], D. De Pedis[132a], A. De Salvo[132a], U. De Sanctis[164a,164c], A. De Santo[149], J.B. De Vivie De Regie[115], S. Dean[77], D.V. Dedovich[65], J. Degenhardt[120], M. Dehchar[118], C. Del Papa[164a,164c], J. Del Peso[80], T. Del Prete[122a,122b], M. Deliyergiyev[74], A. Dell'Acqua[29], L. Dell'Asta[89a,89b], M. Della Pietra[102a,i], D. della Volpe[102a,102b], M. Delmastro[29], P. Delpierre[83], N. Delruelle[29], P.A. Delsart[55], C. Deluca[148], S. Demers[175], M. Demichev[65], B. Demirkoz[11,k], J. Deng[163], S.P. Denisov[128], D. Derendarz[38], J.E. Derkaoui[135d], F. Derue[78], P. Dervan[73], K. Desch[20], E. Devetak[148], P.O. Deviveiros[158], A. Dewhurst[129], B. DeWilde[148], S. Dhaliwal[158], R. Dhullipudi[24,l], A. Di Ciaccio[133a,133b], L. Di Ciaccio[4], A. Di Girolamo[29], B. Di Girolamo[29], S. Di Luise[134a,134b], A. Di Mattia[88], B. Di Micco[29], R. Di Nardo[133a,133b], A. Di Simone[133a,133b], R. Di Sipio[19a,19b], M.A. Diaz[31a], F. Diblen[18c], E.B. Diehl[87], J. Dietrich[41], T.A. Dietzsch[58a], S. Diglio[115], K. Dindar Yagci[39], J. Dingfelder[20], C. Dionisi[132a,132b], P. Dita[25a], S. Dita[25a], F. Dittus[29], F. Djama[83], T. Djobava[51], M.A.B. do Vale[23a], A. Do Valle Wemans[124a], T.K.O. Doan[4], M. Dobbs[85], R. Dobinson [29,*], D. Dobos[42], E. Dobson[29], M. Dobson[163], J. Dodd[34], C. Doglioni[118], T. Doherty[53], Y. Doi[66,*], J. Dolejsi[126], I. Dolenc[74], Z. Dolezal[126], B.A. Dolgoshein[96,*], T. Dohmae[155], M. Donadelli[23b], M. Donega[120], J. Donini[55], J. Dopke[29], A. Doria[102a], A. Dos Anjos[172], M. Dosil[11], A. Dotti[122a,122b], M.T. Dova[70], J.D. Dowell[17], A.D. Doxiadis[105], A.T. Doyle[53], Z. Drasal[126], J. Drees[174], N. Dressnandt[120], H. Drevermann[29], C. Driouichi[35], M. Dris[9], J. Dubbert[99], T. Dubbs[137], S. Dube[14], E. Duchovni[171], G. Duckeck[98], A. Dudarev[29], F. Dudziak[64], M. Dührssen [29], I.P. Duerdoth[82], L. Duflot[115], M-A. Dufour[85], M. Dunford[29], H. Duran Yildiz[3b], R. Duxfield[139], M. Dwuznik[37], F. Dydak [29], D. Dzahini[55], M. Düren[52], W.L. Ebenstein[44], J. Ebke[98], S. Eckert[48], S. Eckweiler[81], K. Edmonds[81], C.A. Edwards[76], N.C. Edwards[53], W. Ehrenfeld[41], T. Ehrich[99], T. Eifert[29], G. Eigen[13], K. Einsweiler[14], E. Eisenhandler[75], T. Ekelof[166], M. El Kacimi[135c], M. Ellert[166], S. Elles[4], F. Ellinghaus[81], K. Ellis[75], N. Ellis[29], J. Elmsheuser[98], M. Elsing[29], R. Ely[14], D. Emeliyanov[129], R. Engelmann[148], A. Engl[98], B. Epp[62], A. Eppig[87], J. Erdmann[54], A. Ereditato[16], D. Eriksson[146a], J. Ernst[1], M. Ernst[24], J. Ernwein[136], D. Errede[165], S. Errede[165], E. Ertel[81], M. Escalier[115], C. Escobar[167], X. Espinal Curull[11], B. Esposito[47], F. Etienne[83], A.I. Etienvre[136], E. Etzion[153], D. Evangelakou[54], H. Evans[61], L. Fabbri[19a,19b], C. Fabre[29], R.M. Fakhrutdinov[128], S. Falciano[132a], Y. Fang[172], M. Fanti[89a,89b], A. Farbin[7], A. Farilla[134a], J. Farley[148], T. Farooque[158], S.M. Farrington[118], P. Farthouat[29], P. Fassnacht[29], D. Fassouliotis[8], B. Fatholahzadeh[158], A. Favareto[89a,89b], L. Fayard[115], S. Fazio[36a,36b],

R. Febbraro[33], P. Federic[144a], O.L. Fedin[121], W. Fedorko[88], M. Fehling-Kaschek[48], L. Feligioni[83], D. Fellmann[5], C.U. Felzmann[86], C. Feng[32d], E.J. Feng[30], A.B. Fenyuk[128], J. Ferencei[144b], J. Ferland[93], W. Fernando[109], S. Ferrag[53], J. Ferrando[53], V. Ferrara[41], A. Ferrari[166], P. Ferrari[105], R. Ferrari[119a], A. Ferrer[167], M.L. Ferrer[47], D. Ferrere[49], C. Ferretti[87], A. Ferretto Parodi[50a,50b], M. Fiascaris[30], F. Fiedler[81], A. Filipčič[74], A. Filippas[9], F. Filthaut[104], M. Fincke-Keeler[169], M.C.N. Fiolhais[124a,h], L. Fiorini[167], A. Firan[39], G. Fischer[41], P. Fischer [20], M.J. Fisher[109], S.M. Fisher[129], M. Flechl[48], I. Fleck[141], J. Fleckner[81], P. Fleischmann[173], S. Fleischmann[174], T. Flick[174], L.R. Flores Castillo[172], M.J. Flowerdew[99], F. Föhlisch[58a], M. Fokitis[9], T. Fonseca Martin[16], D.A. Forbush[138], A. Formica[136], A. Forti[82], D. Fortin[159a], J.M. Foster[82], D. Fournier[115], A. Foussat[29], A.J. Fowler[44], K. Fowler[137], H. Fox[71], P. Francavilla[122a,122b], S. Franchino[119a,119b], D. Francis[29], T. Frank[171], M. Franklin[57], S. Franz[29], M. Fraternali[119a,119b], S. Fratina[120], S.T. French[27], R. Froeschl[29], D. Froidevaux[29], J.A. Frost[27], C. Fukunaga[156], E. Fullana Torregrosa[29], J. Fuster[167], C. Gabaldon[29], O. Gabizon[171], T. Gadfort[24], S. Gadomski[49], G. Gagliardi[50a,50b], P. Gagnon[61], C. Galea[98], E.J. Gallas[118], M.V. Gallas[29], V. Gallo[16], B.J. Gallop[129], P. Gallus[125], E. Galyaev[40], K.K. Gan[109], Y.S. Gao[143,f], V.A. Gapienko[128], A. Gaponenko[14], F. Garberson[175], M. Garcia-Sciveres[14], C. García[167], J.E. García Navarro[49], R.W. Gardner[30], N. Garelli[29], H. Garitaonandia[105], V. Garonne[29], J. Garvey[17], C. Gatti[47], G. Gaudio[119a], O. Gaumer[49], B. Gaur[141], L. Gauthier[136], I.L. Gavrilenko[94], C. Gay[168], G. Gaycken[20], J-C. Gayde[29], E.N. Gazis[9], P. Ge[32d], C.N.P. Gee[129], D.A.A. Geerts[105], Ch. Geich-Gimbel[20], K. Gellerstedt[146a,146b], C. Gemme[50a], A. Gemmell[53], M.H. Genest[98], S. Gentile[132a,132b], M. George[54], S. George[76], P. Gerlach[174], A. Gershon[153], C. Geweniger[58a], H. Ghazlane[135b], P. Ghez[4], N. Ghodbane[33], B. Giacobbe[19a], S. Giagu[132a,132b], V. Giakoumopoulou[8], V. Giangiobbe[122a,122b], F. Gianotti[29], B. Gibbard[24], A. Gibson[158], S.M. Gibson[29], L.M. Gilbert[118], M. Gilchriese[14], V. Gilewsky[91], D. Gillberg[28], A.R. Gillman[129], D.M. Gingrich[2,e], J. Ginzburg[153], N. Giokaris[8], R. Giordano[102a,102b], F.M. Giorgi[15], P. Giovannini[99], P.F. Giraud[136], D. Giugni[89a], M. Giunta[132a,132b], P. Giusti[19a], B.K. Gjelsten[117], L.K. Gladilin[97], C. Glasman[80], J. Glatzer[48], A. Glazov[41], K.W. Glitza[174], G.L. Glonti[65], J. Godfrey[142], J. Godlewski[29], M. Goebel[41], T. Göpfert[43], C. Goeringer[81], C. Gössling[42], T. Göttfert[99], S. Goldfarb[87], D. Goldin[39], T. Golling[175], S.N. Golovnia[128], A. Gomes[124a,b], L.S. Gomez Fajardo[41], R. Gonçalo[76], J. Goncalves Pinto Firmino Da Costa[41], L. Gonella[20], A. Gonidec[29], S. Gonzalez[172], S. González de la Hoz[167], M.L. Gonzalez Silva[26], S. Gonzalez-Sevilla[49], J.J. Goodson[148], L. Goossens[29], P.A. Gorbounov[95], H.A. Gordon[24], I. Gorelov[103], G. Gorfine[174], B. Gorini[29], E. Gorini[72a,72b], A. Gorišek[74], E. Gornicki[38], S.A. Gorokhov[128], V.N. Goryachev[128], B. Gosdzik[41], M. Gosselink[105], M.I. Gostkin[65], M. Gouanère[4], I. Gough Eschrich[163], M. Gouighri[135a], D. Goujdami[135c], M.P. Goulette[49], A.G. Goussiou[138], C. Goy[4], I. Grabowska-Bold[163,g], V. Grabski[176], P. Grafström[29], C. Grah[174], K-J. Grahn[41], F. Grancagnolo[72a], S. Grancagnolo[15], V. Grassi[148], V. Gratchev[121], N. Grau[34], H.M. Gray[29], J.A. Gray[148], E. Graziani[134a], O.G. Grebenyuk[121], D. Greenfield[129], T. Greenshaw[73], Z.D. Greenwood[24,l], I.M. Gregor[41], P. Grenier[143], J. Griffiths[138], N. Grigalashvili[65], A.A. Grillo[137], S. Grinstein[11], Y.V. Grishkevich[97], J.-F. Grivaz[115], J. Grognuz[29], M. Groh[99], E. Gross[171], J. Grosse-Knetter[54], J. Groth-Jensen[171], K. Grybel[141], V.J. Guarino[5], D. Guest[175], C. Guicheney[33], A. Guida[72a,72b], T. Guillemin[4], S. Guindon[54], H. Guler[85,m], C. Gumpert[43], J. Gunther[125], B. Guo[158], J. Guo[34], A. Gupta[30], Y. Gusakov[65], V.N. Gushchin[128], A. Gutierrez[93], P. Gutierrez[111], N. Guttman[153], O. Gutzwiller[172], C. Guyot[136], C. Gwenlan[118], C.B. Gwilliam[73], A. Haas[143], S. Haas[29], C. Haber[14], R. Hackenburg[24], H.K. Hadavand[39], D.R. Hadley[17], P. Haefner[99], F. Hahn[29], S. Haider[29], Z. Hajduk[38], H. Hakobyan[176], J. Haller[54], K. Hamacher[174], P. Hamal[113], A. Hamilton[49], S. Hamilton[161], H. Han[32a], L. Han[32b], K. Hanagaki[116], M. Hance[120], C. Handel[81], P. Hanke[58a], J.R. Hansen[35], J.B. Hansen[35], J.D. Hansen[35], P.H. Hansen[35], P. Hansson[143], K. Hara[160], G.A. Hare[137], T. Harenberg[174], S. Harkusha[90], D. Harper[87], R.D. Harrington[21], O.M. Harris[138], K. Harrison[17], J. Hartert[48], F. Hartjes[105], T. Haruyama[66], A. Harvey[56], S. Hasegawa[101], Y. Hasegawa[140], S. Hassani[136], M. Hatch[29], D. Hauff[99], S. Haug[16], M. Hauschild[29], R. Hauser[88], M. Havranek[20], B.M. Hawes[118], C.M. Hawkes[17], R.J. Hawkings[29], D. Hawkins[163], T. Hayakawa[67], D Hayden[76], H.S. Hayward[73], S.J. Haywood[129], E. Hazen[21], M. He[32d], S.J. Head[17], V. Hedberg[79], L. Heelan[7], S. Heim[88], B. Heinemann[14], S. Heisterkamp[35], L. Helary[4], M. Heller[115], S. Hellman[146a,146b], D. Hellmich[20], C. Helsens[11], R.C.W. Henderson[71], M. Henke[58a], A. Henrichs[54], A.M. Henriques Correia[29], S. Henrot-Versille[115], F. Henry-Couannier[83], C. Hensel[54], T. Henß[174], C.M. Hernandez[7], Y. Hernández Jiménez[167], R. Herrberg[15], A.D. Hershenhorn[152], G. Herten[48], R. Hertenberger[98], L. Hervas[29], N.P. Hessey[105], A. Hidvegi[146a], E. Higón-Rodriguez[167], D. Hill[5,*], J.C. Hill[27], N. Hill[5], K.H. Hiller[41], S. Hillert[20], S.J. Hillier[17], I. Hinchliffe[14], E. Hines[120], M. Hirose[116], F. Hirsch[42], D. Hirschbuehl[174], J. Hobbs[148], N. Hod[153], M.C. Hodgkinson[139], P. Hodgson[139], A. Hoecker[29], M.R. Hoeferkamp[103], J. Hoffman[39], D. Hoffmann[83], M. Hohlfeld[81], M. Holder[141], A. Holmes[118], S.O. Holmgren[146a], T. Holy[127], J.L. Holzbauer[88], Y. Homma[67], T.M. Hong[120], L. Hooft van Huysduynen[108], T. Horazdovsky[127], C. Horn[143], S. Horner[48], K. Horton[118], J-Y. Hostachy[55], S. Hou[151], M.A. Houlden[73], A. Hoummada[135a], J. Howarth[82], D.F. Howell[118], I. Hristova [15], J. Hrivnac[115], I. Hruska[125], T. Hryn'ova[4], P.J. Hsu[175], S.-C. Hsu[14], G.S. Huang[111], Z. Hubacek[127], F. Hubaut[83], F. Huegging[20], T.B. Huffman[118], E.W. Hughes[34], G. Hughes[71], R.E. Hughes-Jones[82], M. Huhtinen[29], P. Hurst[57], M. Hurwitz[14], U. Husemann[41], N. Huseynov[65,n], J. Huston[88], J. Huth[57], G. Iacobucci[49], G. Iakovidis[9], M. Ibbotson[82],

I. Ibragimov[141], R. Ichimiya[67], L. Iconomidou-Fayard[115], J. Idarraga[115], M. Idzik[37], P. Iengo[102a,102b], O. Igonkina[105], Y. Ikegami[66], M. Ikeno[66], Y. Ilchenko[39], D. Iliadis[154], D. Imbault[78], M. Imhaeuser[174], M. Imori[155], T. Ince[20], J. Inigo-Golfin[29], P. Ioannou[8], M. Iodice[134a], G. Ionescu[4], A. Irles Quiles[167], K. Ishii[66], A. Ishikawa[67], M. Ishino[66], R. Ishmukhametov[39], C. Issever[118], S. Istin[18a], Y. Itoh[101], A.V. Ivashin[128], W. Iwanski[38], H. Iwasaki[66], J.M. Izen[40], V. Izzo[102a], B. Jackson[120], J.N. Jackson[73], P. Jackson[143], M.R. Jaekel[29], V. Jain[61], K. Jakobs[48], S. Jakobsen[35], J. Jakubek[127], D.K. Jana[111], E. Jankowski[158], E. Jansen[77], A. Jantsch[99], M. Janus[20], G. Jarlskog[79], L. Jeanty[57], K. Jelen[37], I. Jen-La Plante[30], P. Jenni[29], A. Jeremie[4], P. Jež[35], S. Jézéquel[4], M.K. Jha[19a], H. Ji[172], W. Ji[81], J. Jia[148], Y. Jiang[32b], M. Jimenez Belenguer[41], G. Jin[32b], S. Jin[32a], O. Jinnouchi[157], M.D. Joergensen[35], D. Joffe[39], L.G. Johansen[13], M. Johansen[146a,146b], K.E. Johansson[146a], P. Johansson[139], S. Johnert[41], K.A. Johns[6], K. Jon-And[146a,146b], G. Jones[82], R.W.L. Jones[71], T.W. Jones[77], T.J. Jones[73], O. Jonsson[29], C. Joram[29], P.M. Jorge[124a,b], J. Joseph[14], T. Jovin[12b], X. Ju[130], V. Juranek[125], P. Jussel[62], V.V. Kabachenko[128], S. Kabana[16], M. Kaci[167], A. Kaczmarska[38], P. Kadlecik[35], M. Kado[115], H. Kagan[109], M. Kagan[57], S. Kaiser[99], E. Kajomovitz[152], S. Kalinin[174], L.V. Kalinovskaya[65], S. Kama[39], N. Kanaya[155], M. Kaneda[29], T. Kanno[157], V.A. Kantserov[96], J. Kanzaki[66], B. Kaplan[175], A. Kapliy[30], J. Kaplon[29], D. Kar[43], M. Karagoz[118], M. Karnevskiy[41], K. Karr[5], V. Kartvelishvili[71], A.N. Karyukhin[128], L. Kashif[172], A. Kasmi[39], R.D. Kass[109], A. Kastanas[13], M. Kataoka[4], Y. Kataoka[155], E. Katsoufis[9], J. Katzy[41], V. Kaushik[6], K. Kawagoe[67], T. Kawamoto[155], G. Kawamura[81], M.S. Kayl[105], V.A. Kazanin[107], M.Y. Kazarinov[65], J.R. Keates[82], R. Keeler[169], R. Kehoe[39], M. Keil[54], G.D. Kekelidze[65], M. Kelly[82], J. Kennedy[98], C.J. Kenney[143], M. Kenyon[53], O. Kepka[125], N. Kerschen[29], B.P. Kerševan[74], S. Kersten[174], K. Kessoku[155], C. Ketterer[48], J. Keung[158], M. Khakzad[28], F. Khalil-zada[10], H. Khandanyan[165], A. Khanov[112], D. Kharchenko[65], A. Khodinov[96], A.G. Kholodenko[128], A. Khomich[58a], T.J. Khoo[27], G. Khoriauli[20], A. Khoroshilov[174], N. Khovanskiy[65], V. Khovanskiy[95], E. Khramov[65], J. Khubua[51], H. Kim[7], M.S. Kim[2], P.C. Kim[143], S.H. Kim[160], N. Kimura[170], O. Kind[15], B.T. King[73], M. King[67], R.S.B. King[118], J. Kirk[129], G.P. Kirsch[118], L.E. Kirsch[22], A.E. Kiryunin[99], D. Kisielewska[37], T. Kittelmann[123], A.M. Kiver[128], H. Kiyamura[67], E. Kladiva[144b], J. Klaiber-Lodewigs[42], M. Klein[73], U. Klein[73], K. Kleinknecht[81], M. Klemetti[85], A. Klier[171], A. Klimentov[24], R. Klingenberg[42], E.B. Klinkby[35], T. Klioutchnikova[29], P.F. Klok[104], S. Klous[105], E.-E. Kluge[58a], T. Kluge[73], P. Kluit[105], S. Kluth[99], E. Kneringer[62], J. Knobloch[29], E.B.F.G. Knoops[83], A. Knue[54], B.R. Ko[44], T. Kobayashi[155], M. Kobel[43], M. Kocian[143], A. Kocnar[113], P. Kodys[126], K. Köneke[29], A.C. König[104], S. Koenig[81], L. Köpke[81], F. Koetsveld[104], P. Koevesarki[20], T. Koffas[29], E. Koffeman[105], F. Kohn[54], Z. Kohout[127], T. Kohriki[66], T. Koi[143], T. Kokott[20], G.M. Kolachev[107], H. Kolanoski[15], V. Kolesnikov[65], I. Koletsou[89a], J. Koll[88], D. Kollar[29], M. Kollefrath[48], S.D. Kolya[82], A.A. Komar[94], J.R. Komaragiri[142], Y. Komori[155], T. Kondo[66], T. Kono[41,o], A.I. Kononov[48], R. Konoplich[108,p], N. Konstantinidis[77], A. Kootz[174], S. Koperny[37], S.V. Kopikov[128], K. Korcyl[38], K. Kordas[154], V. Koreshev[128], A. Korn[14], A. Korol[107], I. Korolkov[11], E.V. Korolkova[139], V.A. Korotkov[128], O. Kortner[99], S. Kortner[99], V.V. Kostyukhin[20], M.J. Kotamäki[29], S. Kotov[99], V.M. Kotov[65], A. Kotwal[44], C. Kourkoumelis[8], V. Kouskoura[154], A. Koutsman[105], R. Kowalewski[169], T.Z. Kowalski[37], W. Kozanecki[136], A.S. Kozhin[128], V. Kral[127], V.A. Kramarenko[97], G. Kramberger[74], M.W. Krasny[78], A. Krasznahorkay[108], J. Kraus[88], A. Kreisel[153], F. Krejci[127], J. Kretzschmar[73], N. Krieger[54], P. Krieger[158], K. Kroeninger[54], H. Kroha[99], J. Kroll[120], J. Kroseberg[20], J. Krstic[12a], U. Kruchonak[65], H. Krüger[20], T. Kruker[16], Z.V. Krumshteyn[65], A. Kruth[20], T. Kubota[86], S. Kuehn[48], A. Kugel[58c], T. Kuhl[41], D. Kuhn[62], V. Kukhtin[65], Y. Kulchitsky[90], S. Kuleshov[31b], C. Kummer[98], M. Kuna[78], N. Kundu[118], J. Kunkle[120], A. Kupco[125], H. Kurashige[67], M. Kurata[160], Y.A. Kurochkin[90], V. Kus[125], W. Kuykendall[138], M. Kuze[157], P. Kuzhir[91], O. Kvasnicka[125], J. Kvita[29], R. Kwee[15], A. La Rosa[172], L. La Rotonda[36a,36b], L. Labarga[80], J. Labbe[4], S. Lablak[135a], C. Lacasta[167], F. Lacava[132a,132b], H. Lacker[15], D. Lacour[78], V.R. Lacuesta[167], E. Ladygin[65], R. Lafaye[4], B. Laforge[78], T. Lagouri[80], S. Lai[48], E. Laisne[55], M. Lamanna[29], C.L. Lampen[6], W. Lampl[6], E. Lancon[136], U. Landgraf[48], M.P.J. Landon[75], H. Landsman[152], J.L. Lane[82], C. Lange[41], A.J. Lankford[163], F. Lanni[24], K. Lantzsch[29], S. Laplace[78], C. Lapoire[20], J.F. Laporte[136], T. Lari[89a], A.V. Larionov [128], A. Larner[118], C. Lasseur[29], M. Lassnig[29], P. Laurelli[47], A. Lavorato[118], W. Lavrijsen[14], P. Laycock[73], A.B. Lazarev[65], O. Le Dortz[78], E. Le Guirriec[83], C. Le Maner[158], E. Le Menedeu[136], C. Lebel[93], T. LeCompte[5], F. Ledroit-Guillon[55], H. Lee[105], J.S.H. Lee[150], S.C. Lee[151], L. Lee[175], M. Lefebvre[169], M. Legendre[136], A. Leger[49], B.C. LeGeyt[120], F. Legger[98], C. Leggett[14], M. Lehmacher[20], G. Lehmann Miotto[29], X. Lei[6], M.A.L. Leite[23b], R. Leitner[126], D. Lellouch[171], J. Lellouch[78], M. Leltchouk[34], V. Lendermann[58a], K.J.C. Leney[145b], T. Lenz[174], G. Lenzen[174], B. Lenzi[29], K. Leonhardt[43], S. Leontsinis[9], C. Leroy[93], J-R. Lessard[169], J. Lesser[146a], C.G. Lester[27], A. Leung Fook Cheong[172], J. Levêque[4], D. Levin[87], L.J. Levinson[171], M.S. Levitski[128], M. Lewandowska[21], A. Lewis[118], G.H. Lewis[108], A.M. Leyko[20], M. Leyton[15], B. Li[83], H. Li[172], S. Li[32b,d], X. Li[87], Z. Liang[39], Z. Liang[118,q], B. Liberti[133a], P. Lichard[29], M. Lichtnecker[98], K. Lie[165], W. Liebig[13], R. Lifshitz[152], J.N. Lilley[17], C. Limbach[20], A. Limosani[86], M. Limper[63], S.C. Lin[151,r], F. Linde[105], J.T. Linnemann[88], E. Lipeles[120], L. Lipinsky[125], A. Lipniacka[13], T.M. Liss[165], D. Lissauer[24], A. Lister[49], A.M. Litke[137], C. Liu[28], D. Liu[151,s], H. Liu[87], J.B. Liu[87], M. Liu[32b], S. Liu[2], Y. Liu[32b], M. Livan[119a,119b], S.S.A. Livermore[118], A. Lleres[55], J. Llorente Merino[80], S.L. Lloyd[75], E. Lobodzinska[41], P. Loch[6], W.S. Lockman[137], S. Lockwitz[175],

T. Loddenkoetter[20], F.K. Loebinger[82], A. Loginov[175], C.W. Loh[168], T. Lohse[15], K. Lohwasser[48], M. Lokajicek[125], J. Loken [118], V.P. Lombardo[4], R.E. Long[71], L. Lopes[124a,b], D. Lopez Mateos[57], M. Losada[162], P. Loscutoff[14], F. Lo Sterzo[132a,132b], M.J. Losty[159a], X. Lou[40], A. Lounis[115], K.F. Loureiro[162], J. Love[21], P.A. Love[71], A.J. Lowe[143,f], F. Lu[32a], H.J. Lubatti[138], C. Luci[132a,132b], A. Lucotte[55], A. Ludwig[43], D. Ludwig[41], I. Ludwig[48], J. Ludwig[48], F. Luehring[61], G. Luijckx[105], D. Lumb[48], L. Luminari[132a], E. Lund[117], B. Lund-Jensen[147], B. Lundberg[79], J. Lundberg[146a,146b], J. Lundquist[35], M. Lungwitz[81], A. Lupi[122a,122b], G. Lutz[99], D. Lynn[24], J. Lys[14], E. Lytken[79], H. Ma[24], L.L. Ma[172], J.A. Macana Goia[93], G. Maccarrone[47], A. Macchiolo[99], B. Maček[74], J. Machado Miguens[124a], D. Macina[49], R. Mackeprang[35], R.J. Madaras[14], W.F. Mader[43], R. Maenner[58c], T. Maeno[24], P. Mättig[174], S. Mättig[41], P.J. Magalhaes Martins[124a,h], L. Magnoni[29], E. Magradze[54], Y. Mahalalel[153], K. Mahboubi[48], G. Mahout[17], C. Maiani[132a,132b], C. Maidantchik[23a], A. Maio[124a,b], S. Majewski[24], Y. Makida[66], N. Makovec[115], P. Mal[6], Pa. Malecki[38], P. Malecki[38], V.P. Maleev[121], F. Malek[55], U. Mallik[63], D. Malon[5], S. Maltezos[9], V. Malyshev[107], S. Malyukov[29], R. Mameghani[98], J. Mamuzic[12b], A. Manabe[66], L. Mandelli[89a], I. Mandić[74], R. Mandrysch[15], J. Maneira[124a], P.S. Mangeard[88], I.D. Manjavidze[65], A. Mann[54], P.M. Manning[137], A. Manousakis-Katsikakis[8], B. Mansoulie[136], A. Manz[99], A. Mapelli[29], L. Mapelli[29], L. March [80], J.F. Marchand[29], F. Marchese[133a,133b], G. Marchiori[78], M. Marcisovsky[125], A. Marin[21,*], C.P. Marino[61], F. Marroquim[23a], R. Marshall[82], Z. Marshall[29], F.K. Martens[158], S. Marti-Garcia[167], A.J. Martin[175], B. Martin[29], B. Martin[88], F.F. Martin[120], J.P. Martin[93], Ph. Martin[55], T.A. Martin[17], B. Martin dit Latour[49], M. Martinez[11], V. Martinez Outschoorn[57], A.C. Martyniuk[82], M. Marx[82], F. Marzano[132a], A. Marzin[111], L. Masetti[81], T. Mashimo[155], R. Mashinistov[94], J. Masik[82], A.L. Maslennikov[107], I. Massa[19a,19b], G. Massaro[105], N. Massol[4], P. Mastrandrea[132a,132b], A. Mastroberardino[36a,36b], T. Masubuchi[155], M. Mathes[20], P. Matricon[115], H. Matsumoto[155], H. Matsunaga[155], T. Matsushita[67], C. Mattravers[118,c], J.M. Maugain[29], S.J. Maxfield[73], D.A. Maximov[107], E.N. May[5], A. Mayne[139], R. Mazini[151], M. Mazur[20], M. Mazzanti[89a], E. Mazzoni[122a,122b], S.P. Mc Kee[87], A. McCarn[165], R.L. McCarthy[148], T.G. McCarthy[28], N.A. McCubbin[129], K.W. McFarlane[56], J.A. Mcfayden[139], H. McGlone[53], G. Mchedlidze[51], R.A. McLaren[29], T. Mclaughlan[17], S.J. McMahon[129], R.A. McPherson[169,j], A. Meade[84], J. Mechnich[105], M. Mechtel[174], M. Medinnis[41], R. Meera-Lebbai[111], T. Meguro[116], R. Mehdiyev[93], S. Mehlhase[35], A. Mehta[73], K. Meier[58a], J. Meinhardt[48], B. Meirose[79], C. Melachrinos[30], B.R. Mellado Garcia[172], L. Mendoza Navas[162], Z. Meng[151,s], A. Mengarelli[19a,19b], S. Menke[99], C. Menot[29], E. Meoni[11], K.M. Mercurio[57], P. Mermod[118], L. Merola[102a,102b], C. Meroni[89a], F.S. Merritt[30], A. Messina[29], J. Metcalfe[103], A.S. Mete[64], S. Meuser[20], C. Meyer[81], J-P. Meyer[136], J. Meyer[173], J. Meyer[54], T.C. Meyer[29], W.T. Meyer[64], J. Miao[32d], S. Michal[29], L. Micu[25a], R.P. Middleton[129], P. Miele[29], S. Migas[73], L. Mijović[41], G. Mikenberg[171], M. Mikestikova[125], M. Mikuž[74], D.W. Miller[143], R.J. Miller[88], W.J. Mills[168], C. Mills[57], A. Milov[171], D.A. Milstead[146a,146b], D. Milstein[171], A.A. Minaenko[128], M. Miñano[167], I.A. Minashvili[65], A.I. Mincer[108], B. Mindur[37], M. Mineev[65], Y. Ming[130], L.M. Mir[11], G. Mirabelli[132a], L. Miralles Verge[11], A. Misiejuk[76], J. Mitrevski[137], G.Y. Mitrofanov[128], V.A. Mitsou[167], S. Mitsui[66], P.S. Miyagawa[82], K. Miyazaki[67], J.U. Mjörnmark[79], T. Moa[146a,146b], P. Mockett[138], S. Moed[57], V. Moeller[27], K. Mönig[41], N. Möser[20], S. Mohapatra[148], W. Mohr[48], S. Mohrdieck-Möck[99], A.M. Moisseev[128,*], R. Moles-Valls[167], J. Molina-Perez[29], J. Monk[77], E. Monnier[83], S. Montesano[89a,89b], F. Monticelli[70], S. Monzani[19a,19b], R.W. Moore[2], G.F. Moorhead[86], C. Mora Herrera[49], A. Moraes[53], A. Morais[124a,b], N. Morange[136], J. Morel[54], G. Morello[36a,36b], D. Moreno[81], M. Moreno Llácer[167], P. Morettini[50a], M. Morii[57], J. Morin[75], Y. Morita[66], A.K. Morley[29], G. Mornacchi[29], M-C. Morone[49], S.V. Morozov[96], J.D. Morris[75], L. Morvaj[101], H.G. Moser[99], M. Mosidze[51], J. Moss[109], R. Mount[143], E. Mountricha[136], S.V. Mouraviev[94], E.J.W. Moyse[84], M. Mudrinic[12b], F. Mueller[58a], J. Mueller[123], K. Mueller[20], T.A. Müller[98], D. Muenstermann[29], A. Muir[168], Y. Munwes[153], K. Murakami[66], W.J. Murray[129], I. Mussche[105], E. Musto[102a,102b], A.G. Myagkov[128], M. Myska[125], J. Nadal[11], K. Nagai[160], K. Nagano[66], Y. Nagasaka[60], A.M. Nairz[29], Y. Nakahama[29], K. Nakamura[155], I. Nakano[110], G. Nanava[20], A. Napier[161], M. Nash[77,c], N.R. Nation[21], T. Nattermann[20], T. Naumann[41], G. Navarro[162], H.A. Neal[87], E. Nebot[80], P.Yu. Nechaeva[94], A. Negri[119a,119b], G. Negri[29], S. Nektarijevic[49], S. Nelson[143], T.K. Nelson[143], S. Nemecek[125], P. Nemethy[108], A.A. Nepomuceno[23a], M. Nessi[29,t], S.Y. Nesterov[121], M.S. Neubauer[165], A. Neusiedl[81], R.M. Neves[108], P. Nevski[24], P.R. Newman[17], V. Nguyen Thi Hong[136], R.B. Nickerson[118], R. Nicolaidou[136], L. Nicolas[139], B. Nicquevert[29], F. Niedercorn[115], J. Nielsen[137], T. Niinikoski[29], A. Nikiforov[15], V. Nikolaenko[128], K. Nikolaev[65], I. Nikolic-Audit[78], K. Nikolics[49], K. Nikolopoulos[24], H. Nilsen[48], P. Nilsson[7], Y. Ninomiya [155], A. Nisati[132a], T. Nishiyama[67], R. Nisius[99], L. Nodulman[5], M. Nomachi[116], I. Nomidis[154], M. Nordberg[29], B. Nordkvist[146a,146b], P.R. Norton[129], J. Novakova[126], M. Nozaki[66], M. Nožička[41], L. Nozka[113], I.M. Nugent[159a], A.-E. Nuncio-Quiroz[20], G. Nunes Hanninger[86], T. Nunnemann[98], E. Nurse[77], T. Nyman[29], B.J. O'Brien[45], S.W. O'Neale[17,*], D.C. O'Neil[142], V. O'Shea[53], F.G. Oakham[28,e], H. Oberlack[99], J. Ocariz[78], A. Ochi[67], S. Oda[155], S. Odaka[66], J. Odier[83], H. Ogren[61], A. Oh[82], S.H. Oh[44], C.C. Ohm[146a,146b], T. Ohshima[101], H. Ohshita[140], T.K. Ohska[66], T. Ohsugi[59], S. Okada[67], H. Okawa[163], Y. Okumura[101], T. Okuyama[155], M. Olcese[50a], A.G. Olchevski[65], M. Oliveira[124a,h], D. Oliveira Damazio[24], E. Oliver Garcia[167], D. Olivito[120], A. Olszewski[38], J. Olszowska[38], C. Omachi[67], A. Onofre[124a,u], P.U.E. Onyisi[30], C.J. Oram[159a], M.J. Oreglia[30], Y. Oren[153],

D. Orestano[134a,134b], I. Orlov[107], C. Oropeza Barrera[53], R.S. Orr[158], B. Osculati[50a,50b], R. Ospanov[120], C. Osuna[11], G. Otero y Garzon[26], J.P Ottersbach[105], M. Ouchrif[135d], F. Ould-Saada[117], A. Ouraou[136], Q. Ouyang[32a], M. Owen[82], S. Owen[139], V.E. Ozcan[18a], N. Ozturk[7], A. Pacheco Pages[11], C. Padilla Aranda[11], S. Pagan Griso[14], E. Paganis[139], F. Paige[24], K. Pajchel[117], S. Palestini[29], D. Pallin[33], A. Palma[124a,b], J.D. Palmer[17], Y.B. Pan[172], E. Panagiotopoulou[9], B. Panes[31a], N. Panikashvili[87], S. Panitkin[24], D. Pantea[25a], M. Panuskova[125], V. Paolone[123], A. Papadelis[146a], Th.D. Papadopoulou[9], A. Paramonov[5], W. Park[24,v], M.A. Parker[27], F. Parodi[50a,50b], J.A. Parsons[34], U. Parzefall[48], E. Pasqualucci[132a], A. Passeri[134a], F. Pastore[134a,134b], Fr. Pastore[29], G. Pásztor [49,w], S. Pataraia[172], N. Patel[150], J.R. Pater[82], S. Patricelli[102a,102b], T. Pauly[29], M. Pecsy[144a], M.I. Pedraza Morales[172], S.V. Peleganchuk[107], H. Peng[172], R. Pengo[29], A. Penson[34], J. Penwell[61], M. Perantoni[23a], K. Perez[34,x], T. Perez Cavalcanti[41], E. Perez Codina[11], M.T. Pérez García-Estañ[167], V. Perez Reale[34], L. Perini[89a,89b], H. Pernegger[29], R. Perrino[72a], P. Perrodo[4], S. Persembe[3a], V.D. Peshekhonov[65], O. Peters[105], B.A. Petersen[29], J. Petersen[29], T.C. Petersen[35], E. Petit[83], A. Petridis[154], C. Petridou[154], E. Petrolo[132a], F. Petrucci[134a,134b], D. Petschull[41], M. Petteni[142], R. Pezoa[31b], A. Phan[86], A.W. Phillips[27], P.W. Phillips[129], G. Piacquadio[29], E. Piccaro[75], M. Piccinini[19a,19b], A. Pickford[53], S.M. Piec[41], R. Piegaia[26], J.E. Pilcher[30], A.D. Pilkington[82], J. Pina[124a,b], M. Pinamonti[164a,164c], A. Pinder[118], J.L. Pinfold[2], J. Ping[32c], B. Pinto[124a,b], O. Pirotte[29], C. Pizio[89a,89b], R. Placakyte[41], M. Plamondon[169], W.G. Plano[82], M.-A. Pleier[24], A.V. Pleskach[128], A. Poblaguev[24], S. Poddar[58a], F. Podlyski[33], L. Poggioli[115], T. Poghosyan[20], M. Pohl[49], F. Polci[55], G. Polesello[119a], A. Policicchio[138], A. Polini[19a], J. Poll[75], V. Polychronakos[24], D.M. Pomarede[136], D. Pomeroy[22], K. Pommès[29], L. Pontecorvo[132a], B.G. Pope[88], G.A. Popeneciu[25a], D.S. Popovic[12a], A. Poppleton[29], R. Porter[163], C. Posch[21], G.E. Pospelov[99], S. Pospisil[127], I.N. Potrap[99], C.J. Potter[149], C.T. Potter[114], G. Poulard[29], J. Poveda[172], R. Prabhu[77], P. Pralavorio[83], S. Prasad[57], R. Pravahan[7], S. Prell[64], K. Pretzl[16], L. Pribyl[29], D. Price[61], L.E. Price[5], M.J. Price[29], P.M. Prichard[73], D. Prieur[123], M. Primavera[72a], K. Prokofiev[108], F. Prokoshin[31b], S. Protopopescu[24], J. Proudfoot[5], X. Prudent[43], H. Przysiezniak[4], S. Psoroulas[20], E. Ptacek[114], J. Purdham[87], M. Purohit[24,v], P. Puzo[115], Y. Pylypchenko[117], J. Qian[87], Z. Qian[83], Z. Qin[41], A. Quadt[54], D.R. Quarrie[14], W.B. Quayle[172], F. Quinonez[31a], M. Raas[104], V. Radescu[58b], B. Radics[20], T. Rador[18a], F. Ragusa[89a,89b], G. Rahal[177], A.M. Rahimi[109], D. Rahm[24], S. Rajagopalan[24], M. Rammensee[48], M. Rammes[141], M. Ramstedt[146a,146b], K. Randrianarivony[28], P.N. Ratoff[71], F. Rauscher[98], E. Rauter[99], M. Raymond[29], A.L. Read[117], D.M. Rebuzzi[119a,119b], A. Redelbach[173], G. Redlinger[24], R. Reece[120], K. Reeves[40], A. Reichold[105], E. Reinherz-Aronis[153], A. Reinsch[114], I. Reisinger[42], D. Reljic[12a], C. Rembser[29], Z.L. Ren[151], A. Renaud[115], P. Renkel[39], M. Rescigno[132a], S. Resconi[89a], B. Resende[136], P. Reznicek[98], R. Rezvani[158], A. Richards[77], R. Richter[99], E. Richter-Was[38,y], M. Ridel[78], S. Rieke[81], M. Rijpstra[105], M. Rijssenbeek[148], A. Rimoldi[119a,119b], L. Rinaldi[19a], R.R. Rios[39], I. Riu[11], G. Rivoltella[89a,89b], F. Rizatdinova[112], E. Rizvi[75], S.H. Robertson[85,j], A. Robichaud-Veronneau[49], D. Robinson[27], J.E.M. Robinson[77], M. Robinson[114], A. Robson[53], J.G. Rocha de Lima[106], C. Roda[122a,122b], D. Roda Dos Santos[29], S. Rodier[80], D. Rodriguez[162], A. Roe[54], S. Roe[29], O. Røhne[117], V. Rojo[1], S. Rolli[161], A. Romaniouk[96], V.M. Romanov[65], G. Romeo[26], D. Romero Maltrana[31a], L. Roos[78], E. Ros[167], S. Rosati[132a,132b], K. Rosbach[49], M. Rose[76], G.A. Rosenbaum[158], E.I. Rosenberg[64], P.L. Rosendahl[13], L. Rosselet[49], V. Rossetti[11], E. Rossi[102a,102b], L.P. Rossi[50a], L. Rossi[89a,89b], M. Rotaru[25a], I. Roth[171], J. Rothberg[138], D. Rousseau[115], C.R. Royon[136], A. Rozanov[83], Y. Rozen[152], X. Ruan[115], I. Rubinskiy[41], B. Ruckert[98], N. Ruckstuhl[105], V.I. Rud[97], C. Rudolph[43], G. Rudolph[62], F. Rühr[6], F. Ruggieri[134a,134b], A. Ruiz-Martinez[64], E. Rulikowska-Zarebska[37], V. Rumiantsev[91,*], L. Rumyantsev[65], K. Runge[48], O. Runolfsson[20], Z. Rurikova[48], N.A. Rusakovich[65], D.R. Rust[61], J.P. Rutherfoord[6], C. Ruwiedel[14], P. Ruzicka[125], Y.F. Ryabov[121], V. Ryadovikov[128], P. Ryan[88], M. Rybar[126], G. Rybkin[115], N.C. Ryder[118], S. Rzaeva[10], A.F. Saavedra[150], I. Sadeh[153], H.F-W. Sadrozinski[137], R. Sadykov[65], F. Safai Tehrani[132a,132b], H. Sakamoto[155], G. Salamanna[75], A. Salamon[133a], M. Saleem[111], D. Salihagic[99], A. Salnikov[143], J. Salt[167], B.M. Salvachua Ferrando[5], D. Salvatore[36a,36b], F. Salvatore[149], A. Salvucci[104], A. Salzburger[29], D. Sampsonidis[154], B.H. Samset[117], A. Sanchez[102a,102b], H. Sandaker[13], H.G. Sander[81], M.P. Sanders[98], M. Sandhoff[174], T. Sandoval[27], R. Sandstroem[99], S. Sandvoss[174], D.P.C. Sankey[129], A. Sansoni[47], C. Santamarina Rios[85], C. Santoni[33], R. Santonico[133a,133b], H. Santos[124a], J.G. Saraiva[124a,b], T. Sarangi[172], E. Sarkisyan-Grinbaum[7], F. Sarri[122a,122b], G. Sartisohn[174], O. Sasaki[66], T. Sasaki[66], N. Sasao[68], I. Satsounkevitch[90], G. Sauvage[4], E. Sauvan[4], J.B. Sauvan[115], P. Savard[158,e], V. Savinov[123], D.O. Savu[29], P. Savva [9], L. Sawyer[24,l], D.H. Saxon[53], L.P. Says[33], C. Sbarra[19a,19b], A. Sbrizzi[19a,19b], O. Scallon[93], D.A. Scannicchio[163], J. Schaarschmidt[115], P. Schacht[99], U. Schäfer[81], S. Schaepe[20], S. Schaetzel[58b], A.C. Schaffer[115], D. Schaile[98], R.D. Schamberger[148], A.G. Schamov[107], V. Scharf[58a], V.A. Schegelsky[121], D. Scheirich[87], M. Schernau[163], M.I. Scherzer[14], C. Schiavi[50a,50b], J. Schieck[98], M. Schioppa[36a,36b], S. Schlenker[29], J.L. Schlereth[5], E. Schmidt[48], K. Schmieden[20], C. Schmitt[81], S. Schmitt[58b], M. Schmitz[20], A. Schöning[58b], M. Schott[29], D. Schouten[142], J. Schovancova[125], M. Schram[85], C. Schroeder[81], N. Schroer[58c], S. Schuh[29], G. Schuler[29], J. Schultes[174], H.-C. Schultz-Coulon[58a], H. Schulz[15], J.W. Schumacher[20], M. Schumacher[48], B.A. Schumm[137], Ph. Schune[136], C. Schwanenberger[82], A. Schwartzman[143], Ph. Schwemling[78], R. Schwienhorst[88], R. Schwierz[43], J. Schwindling[136], T. Schwindt[20], W.G. Scott[129], J. Searcy[114], E. Sedykh[121],

E. Segura[11], S.C. Seidel[103], A. Seiden[137], F. Seifert[43], J.M. Seixas[23a], G. Sekhniaidze[102a], D.M. Seliverstov[121], B. Sellden[146a], G. Sellers[73], M. Seman[144b], N. Semprini-Cesari[19a,19b], C. Serfon[98], L. Serin[115], R. Seuster[99], H. Severini[111], M.E. Sevior[86], A. Sfyrla[29], E. Shabalina[54], M. Shamim[114], L.Y. Shan[32a], J.T. Shank[21], Q.T. Shao[86], M. Shapiro[14], P.B. Shatalov[95], L. Shaver[6], C. Shaw[53], K. Shaw[164a,164c], D. Sherman[175], P. Sherwood[77], A. Shibata[108], H. Shichi[101], S. Shimizu[29], M. Shimojima[100], T. Shin[56], A. Shmeleva[94], M.J. Shochet[30], D. Short[118], M.A. Shupe[6], P. Sicho[125], A. Sidoti[132a,132b], A. Siebel[174], F. Siegert[48], J. Siegrist[14], Dj. Sijacki[12a], O. Silbert[171], J. Silva[124a,b], Y. Silver[153], D. Silverstein[143], S.B. Silverstein[146a], V. Simak[127], O. Simard[136], Lj. Simic[12a], S. Simion[115], B. Simmons[77], M. Simonyan[35], P. Sinervo[158], N.B. Sinev[114], V. Sipica[141], G. Siragusa[173], A.N. Sisakyan[65], S.Yu. Sivoklokov[97], J. Sjölin[146a,146b], T.B. Sjursen[13], L.A. Skinnari[14], K. Skovpen[107], P. Skubic[111], N. Skvorodnev[22], M. Slater[17], T. Slavicek[127], K. Sliwa[161], T.J. Sloan[71], J. Sloper[29], V. Smakhtin[171], S.Yu. Smirnov[96], L.N. Smirnova[97], O. Smirnova[79], B.C. Smith[57], D. Smith[143], K.M. Smith[53], M. Smizanska[71], K. Smolek[127], A.A. Snesarev[94], S.W. Snow[82], J. Snow[111], J. Snuverink[105], S. Snyder[24], M. Soares[124a], R. Sobie[169,j], J. Sodomka[127], A. Soffer[153], C.A. Solans[167], M. Solar[127], J. Solc[127], E. Soldatov[96], U. Soldevila[167], E. Solfaroli Camillocci[132a,132b], A.A. Solodkov[128], O.V. Solovyanov[128], J. Sondericker[24], N. Soni[2], V. Sopko[127], B. Sopko[127], M. Sorbi[89a,89b], M. Sosebee[7], A. Soukharev[107], S. Spagnolo[72a,72b], F. Spanò[34], R. Spighi[19a], G. Spigo[29], F. Spila[132a,132b], E. Spiriti[134a], R. Spiwoks[29], M. Spousta[126], T. Spreitzer[158], B. Spurlock[7], R.D. St. Denis[53], T. Stahl[141], J. Stahlman[120], R. Stamen[58a], E. Stanecka[29], R.W. Stanek[5], C. Stanescu[134a], S. Stapnes[117], E.A. Starchenko[128], J. Stark[55], P. Staroba[125], P. Starovoitov[91], A. Staude[98], P. Stavina[144a], G. Stavropoulos[14], G. Steele[53], P. Steinbach[43], P. Steinberg[24], I. Stekl[127], B. Stelzer[142], H.J. Stelzer[41], O. Stelzer-Chilton[159a], H. Stenzel[52], K. Stevenson[75], G.A. Stewart[29], J.A. Stillings[20], T. Stockmanns[20], M.C. Stockton[29], K. Stoerig[48], G. Stoicea[25a], S. Stonjek[99], P. Strachota[126], A.R. Stradling[7], A. Straessner[43], J. Strandberg[147], S. Strandberg[146a,146b], A. Strandlie[117], M. Strang[109], E. Strauss[143], M. Strauss[111], P. Strizenec[144b], R. Ströhmer[173], D.M. Strom[114], J.A. Strong[76,*], R. Stroynowski[39], J. Strube[129], B. Stugu[13], I. Stumer[24,*], J. Stupak[148], P. Sturm[174], D.A. Soh[151,q], D. Su[143], HS. Subramania[2], A. Succurro[11], Y. Sugaya[116], T. Sugimoto[101], C. Suhr[106], K. Suita[67], M. Suk[126], V.V. Sulin[94], S. Sultansoy[3d], T. Sumida[29], X. Sun[55], J.E. Sundermann[48], K. Suruliz[139], S. Sushkov[11], G. Susinno[36a,36b], M.R. Sutton[149], Y. Suzuki[66], M. Svatos[125], Yu.M. Sviridov[128], S. Swedish[168], I. Sykora[144a], T. Sykora[126], B. Szeless[29], J. Sánchez[167], D. Ta[105], K. Tackmann[41], A. Taffard[163], R. Tafirout[159a], A. Taga[117], N. Taiblum[153], Y. Takahashi[101], H. Takai[24], R. Takashima[69], H. Takeda[67], T. Takeshita[140], M. Talby[83], A. Talyshev[107], M.C. Tamsett[24], J. Tanaka[155], R. Tanaka[115], S. Tanaka[131], S. Tanaka[66], Y. Tanaka[100], K. Tani[67], N. Tannoury[83], G.P. Tappern[29], S. Tapprogge[81], D. Tardif[158], S. Tarem[152], F. Tarrade[24], G.F. Tartarelli[89a], P. Tas[126], M. Tasevsky[125], E. Tassi[36a,36b], M. Tatarkhanov[14], C. Taylor[77], F.E. Taylor[92], G.N. Taylor[86], W. Taylor[159b], M. Teixeira Dias Castanheira[75], P. Teixeira-Dias[76], K.K. Temming[48], H. Ten Kate[29], P.K. Teng[151], S. Terada[66], K. Terashi[155], J. Terron[80], M. Terwort[41,o], M. Testa[47], R.J. Teuscher[158,j], J. Thadome[174], J. Therhaag[20], T. Theveneaux-Pelzer[78], M. Thioye[175], S. Thoma[48], J.P. Thomas[17], E.N. Thompson[84], P.D. Thompson[17], P.D. Thompson[158], A.S. Thompson[53], E. Thomson[120], M. Thomson[27], R.P. Thun[87], T. Tic[125], V.O. Tikhomirov[94], Y.A. Tikhonov[107], C.J.W.P. Timmermans[104], P. Tipton[175], F.J. Tique Aires Viegas[29], S. Tisserant[83], J. Tobias[48], B. Toczek[37], T. Todorov[4], S. Todorova-Nova[161], B. Toggerson[163], J. Tojo[66], S. Tokár[144a], K. Tokunaga[67], K. Tokushuku[66], K. Tollefson[88], M. Tomoto[101], L. Tompkins[14], K. Toms[103], G. Tong[32a], A. Tonoyan[13], C. Topfel[16], N.D. Topilin[65], I. Torchiani[29], E. Torrence[114], H. Torres[78], E. Torró Pastor[167], J. Toth[83,w], F. Touchard[83], D.R. Tovey[139], D. Traynor[75], T. Trefzger[173], L. Tremblet[29], A. Tricoli[29], I.M. Trigger[159a], S. Trincaz-Duvoid[78], T.N. Trinh[78], M.F. Tripiana[70], W. Trischuk[158], A. Trivedi[24,v], B. Trocmé[55], C. Troncon[89a], M. Trottier-McDonald[142], A. Trzupek[38], C. Tsarouchas[29], J.C-L. Tseng[118], M. Tsiakiris[105], P.V. Tsiareshka[90], D. Tsionou[4], G. Tsipolitis[9], V. Tsiskaridze[48], E.G. Tskhadadze[51], I.I. Tsukerman[95], V. Tsulaia[14], J.-W. Tsung[20], S. Tsuno[66], D. Tsybychev[148], A. Tua[139], J.M. Tuggle[30], M. Turala[38], D. Turecek[127], I. Turk Cakir[3e], E. Turlay[105], R. Turra[89a,89b], P.M. Tuts[34], A. Tykhonov[74], M. Tylmad[146a,146b], M. Tyndel[129], H. Tyrvainen[29], G. Tzanakos[8], K. Uchida[20], I. Ueda[155], R. Ueno[28], M. Ugland[13], M. Uhlenbrock[20], M. Uhrmacher[54], F. Ukegawa[160], G. Unal[29], D.G. Underwood[5], A. Undrus[24], G. Unel[163], Y. Unno[66], D. Urbaniec[34], E. Urkovsky[153], P. Urrejola[31a], G. Usai[7], M. Uslenghi[119a,119b], L. Vacavant[83], V. Vacek[127], B. Vachon[85], S. Vahsen[14], J. Valenta[125], P. Valente[132a], S. Valentinetti[19a,19b], S. Valkar[126], E. Valladolid Gallego[167], S. Vallecorsa[152], J.A. Valls Ferrer[167], H. van der Graaf[105], E. van der Kraaij[105], R. Van Der Leeuw[105], E. van der Poel[105], D. van der Ster[29], B. Van Eijk[105], N. van Eldik[84], P. van Gemmeren[5], Z. van Kesteren[105], I. van Vulpen[105], W. Vandelli[29], G. Vandoni[29], A. Vaniachine[5], P. Vankov[41], F. Vannucci[78], F. Varela Rodriguez[29], R. Vari[132a], E.W. Varnes[6], D. Varouchas[14], A. Vartapetian[7], K.E. Varvell[150], V.I. Vassilakopoulos[56], F. Vazeille[33], G. Vegni[89a,89b], J.J. Veillet[115], C. Vellidis[8], F. Veloso[124a], R. Veness[29], S. Veneziano[132a], A. Ventura[72a,72b], D. Ventura[138], M. Venturi[48], N. Venturi[16], V. Vercesi[119a], M. Verducci[138], W. Verkerke[105], J.C. Vermeulen[105], A. Vest[43], M.C. Vetterli[142,e], I. Vichou[165], T. Vickey[145b,z], G.H.A. Viehhauser[118], S. Viel[168], M. Villa[19a,19b], M. Villaplana Perez[167], E. Vilucchi[47], M.G. Vincter[28], E. Vinek[29], V.B. Vinogradov[65], M. Virchaux[136,*], J. Virzi[14], O. Vitells[171], M. Viti[41], I. Vivarelli[48], F. Vives Vaque[11],

S. Vlachos[9], M. Vlasak[127], N. Vlasov[20], A. Vogel[20], P. Vokac[127], G. Volpi[47], M. Volpi[86], G. Volpini[89a], H. von der Schmitt[99], J. von Loeben[99], H. von Radziewski[48], E. von Toerne[20], V. Vorobel[126], A.P. Vorobiev[128], V. Vorwerk[11], M. Vos[167], R. Voss[29], T.T. Voss[174], J.H. Vossebeld[73], N. Vranjes[12a], M. Vranjes Milosavljevic[105], V. Vrba[125], M. Vreeswijk[105], T. Vu Anh[81], R. Vuillermet[29], I. Vukotic[115], W. Wagner[174], P. Wagner[120], H. Wahlen[174], J. Wakabayashi[101], J. Walbersloh[42], S. Walch[87], J. Walder[71], R. Walker[98], W. Walkowiak[141], R. Wall[175], P. Waller[73], C. Wang[44], H. Wang[172], H. Wang[32b,aa], J. Wang[151], J. Wang[32d], J.C. Wang[138], R. Wang[103], S.M. Wang[151], A. Warburton[85], C.P. Ward[27], M. Warsinsky[48], P.M. Watkins[17], A.T. Watson[17], M.F. Watson[17], G. Watts[138], S. Watts[82], A.T. Waugh[150], B.M. Waugh[77], J. Weber[42], M. Weber[129], M.S. Weber[16], P. Weber[54], A.R. Weidberg[118], P. Weigell[99], J. Weingarten[54], C. Weiser[48], H. Wellenstein[22], P.S. Wells[29], M. Wen[47], T. Wenaus[24], S. Wendler[123], Z. Weng[151,q], T. Wengler[29], S. Wenig[29], N. Wermes[20], M. Werner[48], P. Werner[29], M. Werth[163], M. Wessels[58a], C. Weydert[55], K. Whalen[28], S.J. Wheeler-Ellis[163], S.P. Whitaker[21], A. White[7], M.J. White[86], S. White[24], S.R. Whitehead[118], D. Whiteson[163], D. Whittington[61], F. Wicek[115], D. Wicke[174], F.J. Wickens[129], W. Wiedenmann[172], M. Wielers[129], P. Wienemann[20], C. Wiglesworth[75], L.A.M. Wiik[48], P.A. Wijeratne[77], A. Wildauer[167], M.A. Wildt[41,o], I. Wilhelm[126], H.G. Wilkens[29], J.Z. Will[98], E. Williams[34], H.H. Williams[120], W. Willis[34], S. Willocq[84], J.A. Wilson[17], M.G. Wilson[143], A. Wilson[87], I. Wingerter-Seez[4], S. Winkelmann[48], F. Winklmeier[29], M. Wittgen[143], M.W. Wolter[38], H. Wolters[124a,h], G. Wooden[118], B.K. Wosiek[38], J. Wotschack[29], M.J. Woudstra[84], K. Wraight[53], C. Wright[53], B. Wrona[73], S.L. Wu[172], X. Wu[49], Y. Wu[32b,ab], E. Wulf[34], R. Wunstorf[42], B.M. Wynne[45], L. Xaplanteris[9], S. Xella[35], S. Xie[48], Y. Xie[32a], C. Xu[32b,ac], D. Xu[139], G. Xu[32a], B. Yabsley[150], S. Yacoob[145b], M. Yamada[66], A. Yamamoto[66], K. Yamamoto[64], S. Yamamoto[155], T. Yamamura[155], J. Yamaoka[44], T. Yamazaki[155], Y. Yamazaki[67], Z. Yan[21], H. Yang[87], U.K. Yang[82], Y. Yang[61], Y. Yang[32a], Z. Yang[146a,146b], S. Yanush[91], W-M. Yao[14], Y. Yao[14], Y. Yasu[66], G.V. Ybeles Smit[130], J. Ye[39], S. Ye[24], M. Yilmaz[3c], R. Yoosoofmiya[123], K. Yorita[170], R. Yoshida[5], C. Young[143], S. Youssef[21], D. Yu[24], J. Yu[7], J. Yu[32c,ac], L. Yuan[32a,ad], A. Yurkewicz[148], V.G. Zaets [128], R. Zaidan[63], A.M. Zaitsev[128], Z. Zajacova[29], Yo.K. Zalite [121], L. Zanello[132a,132b], P. Zarzhitsky[39], A. Zaytsev[107], C. Zeitnitz[174], M. Zeller[175], A. Zemla[38], C. Zendler[20], O. Zenin[128], T. Ženiš[144a], Z. Zenonos[122a,122b], S. Zenz[14], D. Zerwas[115], G. Zevi della Porta[57], Z. Zhan[32d], D. Zhang[32b,aa], H. Zhang[88], J. Zhang[5], X. Zhang[32d], Z. Zhang[115], L. Zhao[108], T. Zhao[138], Z. Zhao[32b], A. Zhemchugov[65], S. Zheng[32a], J. Zhong[151,ae], B. Zhou[87], N. Zhou[163], Y. Zhou[151], C.G. Zhu[32d], H. Zhu[41], J. Zhu[87], Y. Zhu[172], X. Zhuang[98], V. Zhuravlov[99], D. Zieminska[61], R. Zimmermann[20], S. Zimmermann[20], S. Zimmermann[48], M. Ziolkowski[141], R. Zitoun[4], L. Živković[34], V.V. Zmouchko[128,*], G. Zobernig[172], A. Zoccoli[19a,19b], Y. Zolnierowski[4], A. Zsenei[29], M. zur Nedden[15], V. Zutshi[106], L. Zwalinski[29].

[1] University at Albany, Albany NY, United States of America
[2] Department of Physics, University of Alberta, Edmonton AB, Canada
[3] [(a)]Department of Physics, Ankara University, Ankara; [(b)]Department of Physics, Dumlupinar University, Kutahya; [(c)]Department of Physics, Gazi University, Ankara; [(d)]Division of Physics, TOBB University of Economics and Technology, Ankara; [(e)]Turkish Atomic Energy Authority, Ankara, Turkey
[4] LAPP, CNRS/IN2P3 and Université de Savoie, Annecy-le-Vieux, France
[5] High Energy Physics Division, Argonne National Laboratory, Argonne IL, United States of America
[6] Department of Physics, University of Arizona, Tucson AZ, United States of America
[7] Department of Physics, The University of Texas at Arlington, Arlington TX, United States of America
[8] Physics Department, University of Athens, Athens, Greece
[9] Physics Department, National Technical University of Athens, Zografou, Greece
[10] Institute of Physics, Azerbaijan Academy of Sciences, Baku, Azerbaijan
[11] Institut de Física d'Altes Energies and Universitat Autònoma de Barcelona and ICREA, Barcelona, Spain
[12] [(a)]Institute of Physics, University of Belgrade, Belgrade; [(b)]Vinca Institute of Nuclear Sciences, Belgrade, Serbia
[13] Department for Physics and Technology, University of Bergen, Bergen, Norway
[14] Physics Division, Lawrence Berkeley National Laboratory and University of California, Berkeley CA, United States of America
[15] Department of Physics, Humboldt University, Berlin, Germany
[16] Albert Einstein Center for Fundamental Physics and Laboratory for High Energy Physics, University of Bern, Bern, Switzerland
[17] School of Physics and Astronomy, University of Birmingham, Birmingham, United Kingdom
[18] [(a)]Department of Physics, Bogazici University, Istanbul; [(b)]Division of Physics, Dogus University, Istanbul; [(c)]Department of Physics Engineering, Gaziantep University, Gaziantep; [(d)]Department of Physics, Istanbul Technical University, Istanbul, Turkey
[19] [(a)]INFN Sezione di Bologna; [(b)]Dipartimento di Fisica, Università di Bologna, Bologna, Italy
[20] Physikalisches Institut, University of Bonn, Bonn, Germany
[21] Department of Physics, Boston University, Boston MA, United States of America

[22] Department of Physics, Brandeis University, Waltham MA, United States of America
[23] [(a)]Universidade Federal do Rio De Janeiro COPPE/EE/IF, Rio de Janeiro; [(b)]Instituto de Fisica, Universidade de Sao Paulo, Sao Paulo, Brazil
[24] Physics Department, Brookhaven National Laboratory, Upton NY, United States of America
[25] [(a)]National Institute of Physics and Nuclear Engineering, Bucharest; [(b)]University Politehnica Bucharest, Bucharest; [(c)]West University in Timisoara, Timisoara, Romania
[26] Departamento de Física, Universidad de Buenos Aires, Buenos Aires, Argentina
[27] Cavendish Laboratory, University of Cambridge, Cambridge, United Kingdom
[28] Department of Physics, Carleton University, Ottawa ON, Canada
[29] CERN, Geneva, Switzerland
[30] Enrico Fermi Institute, University of Chicago, Chicago IL, United States of America
[31] [(a)]Departamento de Fisica, Pontificia Universidad Católica de Chile, Santiago; [(b)]Departamento de Física, Universidad Técnica Federico Santa María, Valparaíso, Chile
[32] [(a)]Institute of High Energy Physics, Chinese Academy of Sciences, Beijing; [(b)]Department of Modern Physics, University of Science and Technology of China, Anhui; [(c)]Department of Physics, Nanjing University, Jiangsu; [(d)]High Energy Physics Group, Shandong University, Shandong, China
[33] Laboratoire de Physique Corpusculaire, Clermont Université and Université Blaise Pascal and CNRS/IN2P3, Aubiere Cedex, France
[34] Nevis Laboratory, Columbia University, Irvington NY, United States of America
[35] Niels Bohr Institute, University of Copenhagen, Kobenhavn, Denmark
[36] [(a)]INFN Gruppo Collegato di Cosenza; [(b)]Dipartimento di Fisica, Università della Calabria, Arcavata di Rende, Italy
[37] Faculty of Physics and Applied Computer Science, AGH-University of Science and Technology, Krakow, Poland
[38] The Henryk Niewodniczanski Institute of Nuclear Physics, Polish Academy of Sciences, Krakow, Poland
[39] Physics Department, Southern Methodist University, Dallas TX, United States of America
[40] Physics Department, University of Texas at Dallas, Richardson TX, United States of America
[41] DESY, Hamburg and Zeuthen, Germany
[42] Institut für Experimentelle Physik IV, Technische Universität Dortmund, Dortmund, Germany
[43] Institut für Kern- und Teilchenphysik, Technical University Dresden, Dresden, Germany
[44] Department of Physics, Duke University, Durham NC, United States of America
[45] SUPA - School of Physics and Astronomy, University of Edinburgh, Edinburgh, United Kingdom
[46] Fachhochschule Wiener Neustadt, Johannes Gutenbergstrasse 3, 2700 Wiener Neustadt, Austria
[47] INFN Laboratori Nazionali di Frascati, Frascati, Italy
[48] Fakultät für Mathematik und Physik, Albert-Ludwigs-Universität, Freiburg i.Br., Germany
[49] Section de Physique, Université de Genève, Geneva, Switzerland
[50] [(a)]INFN Sezione di Genova; [(b)]Dipartimento di Fisica, Università di Genova, Genova, Italy
[51] Institute of Physics and HEP Institute, Georgian Academy of Sciences and Tbilisi State University, Tbilisi, Georgia
[52] II Physikalisches Institut, Justus-Liebig-Universität Giessen, Giessen, Germany
[53] SUPA - School of Physics and Astronomy, University of Glasgow, Glasgow, United Kingdom
[54] II Physikalisches Institut, Georg-August-Universität, Göttingen, Germany
[55] Laboratoire de Physique Subatomique et de Cosmologie, Université Joseph Fourier and CNRS/IN2P3 and Institut National Polytechnique de Grenoble, Grenoble, France
[56] Department of Physics, Hampton University, Hampton VA, United States of America
[57] Laboratory for Particle Physics and Cosmology, Harvard University, Cambridge MA, United States of America
[58] [(a)]Kirchhoff-Institut für Physik, Ruprecht-Karls-Universität Heidelberg, Heidelberg; [(b)]Physikalisches Institut, Ruprecht-Karls-Universität Heidelberg, Heidelberg; [(c)]ZITI Institut für technische Informatik, Ruprecht-Karls-Universität Heidelberg, Mannheim, Germany
[59] Faculty of Science, Hiroshima University, Hiroshima, Japan
[60] Faculty of Applied Information Science, Hiroshima Institute of Technology, Hiroshima, Japan
[61] Department of Physics, Indiana University, Bloomington IN, United States of America
[62] Institut für Astro- und Teilchenphysik, Leopold-Franzens-Universität, Innsbruck, Austria
[63] University of Iowa, Iowa City IA, United States of America
[64] Department of Physics and Astronomy, Iowa State University, Ames IA, United States of America
[65] Joint Institute for Nuclear Research, JINR Dubna, Dubna, Russia
[66] KEK, High Energy Accelerator Research Organization, Tsukuba, Japan
[67] Graduate School of Science, Kobe University, Kobe, Japan
[68] Faculty of Science, Kyoto University, Kyoto, Japan

[69] Kyoto University of Education, Kyoto, Japan
[70] Instituto de Física La Plata, Universidad Nacional de La Plata and CONICET, La Plata, Argentina
[71] Physics Department, Lancaster University, Lancaster, United Kingdom
[72] [(a)]INFN Sezione di Lecce; [(b)]Dipartimento di Fisica, Università del Salento, Lecce, Italy
[73] Oliver Lodge Laboratory, University of Liverpool, Liverpool, United Kingdom
[74] Department of Physics, Jožef Stefan Institute and University of Ljubljana, Ljubljana, Slovenia
[75] Department of Physics, Queen Mary University of London, London, United Kingdom
[76] Department of Physics, Royal Holloway University of London, Surrey, United Kingdom
[77] Department of Physics and Astronomy, University College London, London, United Kingdom
[78] Laboratoire de Physique Nucléaire et de Hautes Energies, UPMC and Université Paris-Diderot and CNRS/IN2P3, Paris, France
[79] Fysiska institutionen, Lunds universitet, Lund, Sweden
[80] Departamento de Fisica Teorica C-15, Universidad Autonoma de Madrid, Madrid, Spain
[81] Institut für Physik, Universität Mainz, Mainz, Germany
[82] School of Physics and Astronomy, University of Manchester, Manchester, United Kingdom
[83] CPPM, Aix-Marseille Université and CNRS/IN2P3, Marseille, France
[84] Department of Physics, University of Massachusetts, Amherst MA, United States of America
[85] Department of Physics, McGill University, Montreal QC, Canada
[86] School of Physics, University of Melbourne, Victoria, Australia
[87] Department of Physics, The University of Michigan, Ann Arbor MI, United States of America
[88] Department of Physics and Astronomy, Michigan State University, East Lansing MI, United States of America
[89] [(a)]INFN Sezione di Milano; [(b)]Dipartimento di Fisica, Università di Milano, Milano, Italy
[90] B.I. Stepanov Institute of Physics, National Academy of Sciences of Belarus, Minsk, Republic of Belarus
[91] National Scientific and Educational Centre for Particle and High Energy Physics, Minsk, Republic of Belarus
[92] Department of Physics, Massachusetts Institute of Technology, Cambridge MA, United States of America
[93] Group of Particle Physics, University of Montreal, Montreal QC, Canada
[94] P.N. Lebedev Institute of Physics, Academy of Sciences, Moscow, Russia
[95] Institute for Theoretical and Experimental Physics (ITEP), Moscow, Russia
[96] Moscow Engineering and Physics Institute (MEPhI), Moscow, Russia
[97] Skobeltsyn Institute of Nuclear Physics, Lomonosov Moscow State University, Moscow, Russia
[98] Fakultät für Physik, Ludwig-Maximilians-Universität München, München, Germany
[99] Max-Planck-Institut für Physik (Werner-Heisenberg-Institut), München, Germany
[100] Nagasaki Institute of Applied Science, Nagasaki, Japan
[101] Graduate School of Science, Nagoya University, Nagoya, Japan
[102] [(a)]INFN Sezione di Napoli; [(b)]Dipartimento di Scienze Fisiche, Università di Napoli, Napoli, Italy
[103] Department of Physics and Astronomy, University of New Mexico, Albuquerque NM, United States of America
[104] Institute for Mathematics, Astrophysics and Particle Physics, Radboud University Nijmegen/Nikhef, Nijmegen, Netherlands
[105] Nikhef National Institute for Subatomic Physics and University of Amsterdam, Amsterdam, Netherlands
[106] Department of Physics, Northern Illinois University, DeKalb IL, United States of America
[107] Budker Institute of Nuclear Physics (BINP), Novosibirsk, Russia
[108] Department of Physics, New York University, New York NY, United States of America
[109] Ohio State University, Columbus OH, United States of America
[110] Faculty of Science, Okayama University, Okayama, Japan
[111] Homer L. Dodge Department of Physics and Astronomy, University of Oklahoma, Norman OK, United States of America
[112] Department of Physics, Oklahoma State University, Stillwater OK, United States of America
[113] Palacký University, RCPTM, Olomouc, Czech Republic
[114] Center for High Energy Physics, University of Oregon, Eugene OR, United States of America
[115] LAL, Univ. Paris-Sud and CNRS/IN2P3, Orsay, France
[116] Graduate School of Science, Osaka University, Osaka, Japan
[117] Department of Physics, University of Oslo, Oslo, Norway
[118] Department of Physics, Oxford University, Oxford, United Kingdom
[119] [(a)]INFN Sezione di Pavia; [(b)]Dipartimento di Fisica Nucleare e Teorica, Università di Pavia, Pavia, Italy
[120] Department of Physics, University of Pennsylvania, Philadelphia PA, United States of America
[121] Petersburg Nuclear Physics Institute, Gatchina, Russia
[122] [(a)]INFN Sezione di Pisa; [(b)]Dipartimento di Fisica E. Fermi, Università di Pisa, Pisa, Italy
[123] Department of Physics and Astronomy, University of Pittsburgh, Pittsburgh PA, United States of America

[124] [(a)]Laboratorio de Instrumentacao e Fisica Experimental de Particulas - LIP, Lisboa, Portugal; [(b)]Departamento de Fisica Teorica y del Cosmos and CAFPE, Universidad de Granada, Granada, Spain
[125] Institute of Physics, Academy of Sciences of the Czech Republic, Praha, Czech Republic
[126] Faculty of Mathematics and Physics, Charles University in Prague, Praha, Czech Republic
[127] Czech Technical University in Prague, Praha, Czech Republic
[128] State Research Center Institute for High Energy Physics, Protvino, Russia
[129] Particle Physics Department, Rutherford Appleton Laboratory, Didcot, United Kingdom
[130] Physics Department, University of Regina, Regina SK, Canada
[131] Ritsumeikan University, Kusatsu, Shiga, Japan
[132] [(a)]INFN Sezione di Roma I; [(b)]Dipartimento di Fisica, Università La Sapienza, Roma, Italy
[133] [(a)]INFN Sezione di Roma Tor Vergata; [(b)]Dipartimento di Fisica, Università di Roma Tor Vergata, Roma, Italy
[134] [(a)]INFN Sezione di Roma Tre; [(b)]Dipartimento di Fisica, Università Roma Tre, Roma, Italy
[135] [(a)]Faculté des Sciences Ain Chock, Réseau Universitaire de Physique des Hautes Energies - Université Hassan II, Casablanca; [(b)]Centre National de l'Energie des Sciences Techniques Nucleaires, Rabat; [(c)]Université Cadi Ayyad, Faculté des sciences Semlalia Département de Physique, B.P. 2390 Marrakech 40000; [(d)]Faculté des Sciences, Université Mohamed Premier and LPTPM, Oujda; [(e)]Faculté des Sciences, Université Mohammed V, Rabat, Morocco
[136] DSM/IRFU (Institut de Recherches sur les Lois Fondamentales de l'Univers), CEA Saclay (Commissariat a l'Energie Atomique), Gif-sur-Yvette, France
[137] Santa Cruz Institute for Particle Physics, University of California Santa Cruz, Santa Cruz CA, United States of America
[138] Department of Physics, University of Washington, Seattle WA, United States of America
[139] Department of Physics and Astronomy, University of Sheffield, Sheffield, United Kingdom
[140] Department of Physics, Shinshu University, Nagano, Japan
[141] Fachbereich Physik, Universität Siegen, Siegen, Germany
[142] Department of Physics, Simon Fraser University, Burnaby BC, Canada
[143] SLAC National Accelerator Laboratory, Stanford CA, United States of America
[144] [(a)]Faculty of Mathematics, Physics & Informatics, Comenius University, Bratislava; [(b)]Department of Subnuclear Physics, Institute of Experimental Physics of the Slovak Academy of Sciences, Kosice, Slovak Republic
[145] [(a)]Department of Physics, University of Johannesburg, Johannesburg; [(b)]School of Physics, University of the Witwatersrand, Johannesburg, South Africa
[146] [(a)]Department of Physics, Stockholm University; [(b)]The Oskar Klein Centre, Stockholm, Sweden
[147] Physics Department, Royal Institute of Technology, Stockholm, Sweden
[148] Department of Physics and Astronomy, Stony Brook University, Stony Brook NY, United States of America
[149] Department of Physics and Astronomy, University of Sussex, Brighton, United Kingdom
[150] School of Physics, University of Sydney, Sydney, Australia
[151] Institute of Physics, Academia Sinica, Taipei, Taiwan
[152] Department of Physics, Technion: Israel Inst. of Technology, Haifa, Israel
[153] Raymond and Beverly Sackler School of Physics and Astronomy, Tel Aviv University, Tel Aviv, Israel
[154] Department of Physics, Aristotle University of Thessaloniki, Thessaloniki, Greece
[155] International Center for Elementary Particle Physics and Department of Physics, The University of Tokyo, Tokyo, Japan
[156] Graduate School of Science and Technology, Tokyo Metropolitan University, Tokyo, Japan
[157] Department of Physics, Tokyo Institute of Technology, Tokyo, Japan
[158] Department of Physics, University of Toronto, Toronto ON, Canada
[159] [(a)]TRIUMF, Vancouver BC; [(b)]Department of Physics and Astronomy, York University, Toronto ON, Canada
[160] Institute of Pure and Applied Sciences, University of Tsukuba, Ibaraki, Japan
[161] Science and Technology Center, Tufts University, Medford MA, United States of America
[162] Centro de Investigaciones, Universidad Antonio Narino, Bogota, Colombia
[163] Department of Physics and Astronomy, University of California Irvine, Irvine CA, United States of America
[164] [(a)]INFN Gruppo Collegato di Udine; [(b)]ICTP, Trieste; [(c)]Dipartimento di Fisica, Università di Udine, Udine, Italy
[165] Department of Physics, University of Illinois, Urbana IL, United States of America
[166] Department of Physics and Astronomy, University of Uppsala, Uppsala, Sweden
[167] Instituto de Física Corpuscular (IFIC) and Departamento de Física Atómica, Molecular y Nuclear and Departamento de Ingenierá Electrónica and Instituto de Microelectrónica de Barcelona (IMB-CNM), University of Valencia and CSIC, Valencia, Spain
[168] Department of Physics, University of British Columbia, Vancouver BC, Canada

[169] Department of Physics and Astronomy, University of Victoria, Victoria BC, Canada
[170] Waseda University, Tokyo, Japan
[171] Department of Particle Physics, The Weizmann Institute of Science, Rehovot, Israel
[172] Department of Physics, University of Wisconsin, Madison WI, United States of America
[173] Fakultät für Physik und Astronomie, Julius-Maximilians-Universität, Würzburg, Germany
[174] Fachbereich C Physik, Bergische Universität Wuppertal, Wuppertal, Germany
[175] Department of Physics, Yale University, New Haven CT, United States of America
[176] Yerevan Physics Institute, Yerevan, Armenia
[177] Domaine scientifique de la Doua, Centre de Calcul CNRS/IN2P3, Villeurbanne Cedex, France
[a] Also at Laboratorio de Instrumentacao e Fisica Experimental de Particulas - LIP, Lisboa, Portugal
[b] Also at Faculdade de Ciencias and CFNUL, Universidade de Lisboa, Lisboa, Portugal
[c] Also at Particle Physics Department, Rutherford Appleton Laboratory, Didcot, United Kingdom
[d] Also at CPPM, Aix-Marseille Université and CNRS/IN2P3, Marseille, France
[e] Also at TRIUMF, Vancouver BC, Canada
[f] Also at Department of Physics, California State University, Fresno CA, United States of America
[g] Also at Faculty of Physics and Applied Computer Science, AGH-University of Science and Technology, Krakow, Poland
[h] Also at Department of Physics, University of Coimbra, Coimbra, Portugal
[i] Also at Università di Napoli Parthenope, Napoli, Italy
[j] Also at Institute of Particle Physics (IPP), Canada
[k] Also at Department of Physics, Middle East Technical University, Ankara, Turkey
[l] Also at Louisiana Tech University, Ruston LA, United States of America
[m] Also at Group of Particle Physics, University of Montreal, Montreal QC, Canada
[n] Also at Institute of Physics, Azerbaijan Academy of Sciences, Baku, Azerbaijan
[o] Also at Institut für Experimentalphysik, Universität Hamburg, Hamburg, Germany
[p] Also at Manhattan College, New York NY, United States of America
[q] Also at School of Physics and Engineering, Sun Yat-sen University, Guanzhou, China
[r] Also at Academia Sinica Grid Computing, Institute of Physics, Academia Sinica, Taipei, Taiwan
[s] Also at High Energy Physics Group, Shandong University, Shandong, China
[t] Also at Section de Physique, Université de Genève, Geneva, Switzerland
[u] Also at Departamento de Fisica, Universidade de Minho, Braga, Portugal
[v] Also at Department of Physics and Astronomy, University of South Carolina, Columbia SC, United States of America
[w] Also at KFKI Research Institute for Particle and Nuclear Physics, Budapest, Hungary
[x] Also at California Institute of Technology, Pasadena CA, United States of America
[y] Also at Institute of Physics, Jagiellonian University, Krakow, Poland
[z] Also at Department of Physics, Oxford University, Oxford, United Kingdom
[aa] Also at Institute of Physics, Academia Sinica, Taipei, Taiwan
[ab] Also at Department of Physics, The University of Michigan, Ann Arbor MI, United States of America
[ac] Also at DSM/IRFU (Institut de Recherches sur les Lois Fondamentales de l'Univers), CEA Saclay (Commissariat a l'Energie Atomique), Gif-sur-Yvette, France
[ad] Also at Laboratoire de Physique Nucléaire et de Hautes Energies, UPMC and Université Paris-Diderot and CNRS/IN2P3, Paris, France
[ae] Also at Department of Physics, Nanjing University, Jiangsu, China
* Deceased